# Design and Construction of a two Lane Traffic Light

Engr. Emmanuel Omosigho

Department of Electrical/Electronic Engineering Technology, National Institute of Construction Technology and Management, Uromi, Edo State, Nigeria.

e.omosigho@nict.edu.ng

#### **Abstract**

This project details the design and construction of a two-lane traffic light model using an Arduino Uno microcontroller. With increased urban traffic, effective traffic control systems have become crucial. The primary objective was to create a functional, cost-effective traffic light system for educational purposes or real-world application scaling. The project comprises four units: power supply, control, traffic light, and wiring/interconnection. The power supply unit, featuring a 12V power adapter and LM7805 voltage regulator, ensured a stable 5V output for the Arduino and other components. The control unit, based on the Arduino Uno, was programmed to manage traffic light timing and sequences. The traffic light unit includes LEDs configured as standard red, yellow, and green signals for both main and adjacent roads, with current-limiting resistors for safe operation. The wiring unit ensures proper connection and communication between components. Using the Arduino IDE, the traffic light sequences were programmed to alternate between the main and adjacent roads, allowing vehicles from one road to proceed while the others wait. This model demonstrates the feasibility of microcontroller-based traffic management systems and highlights the potential of Arduino-based solutions as flexible, economical alternatives to traditional traffic light systems. The project serves as both an educational tool and a prototype for developing intelligent traffic management systems.

Key Words: LED Traffic Lights, Arduino Uno, Traffic Light System, Microcontroller

# I. Introduction

Traffic management is a critical component of urban planning and public safety. With the rapid increase in vehicular traffic due to urbanization and population growth, effective traffic control systems have become essential to ensure the smooth flow of vehicles and the safety of both motorists and pedestrians. Over the years, traffic congestion has been a cause for concern in the society due to its negative effects like stress to commuters, release of more toxic fumes into the atmosphere and loss of man hour (Uzondu et al., 2018). Traffic lights, or traffic signals, play a pivotal role in regulating traffic at intersections, helping to prevent accidents and reduce congestion. They are positioned at junctions, intersections, "X" roads, pedestrian crossings etc. and alternate the priority of who has to wait and who has to go (Parkhi et al., 2016; Ghazal and ElKhatib, 2016; Rotake and Karmore, 2012; Tubaishatr et al., 2007; Kham and Myat, 2014; Rao, 2019).

The concept of traffic control dates back to ancient times, but the first manually operated gas-lit traffic signal was installed in London in 1868 by J.P. Knight, a railway signaling engineer (Tolulope and Patrick, 2014). This pioneering traffic signal featured semaphore arms and was manually operated by a police officer stationed nearby. Despite its innovation, it was short-lived, operating for only about a month due to its susceptibility to gas leaks and the subsequent explosion that occurred shortly after its installation. However, it was not until the advent of the automobile in the early 20th century that traffic lights became a widespread necessity. The first electric traffic light was installed in Cleveland, Ohio, in 1914 (Tolulope and

Patrick, 2014). Since then, traffic lights have evolved significantly, incorporating advanced technologies to improve their efficiency and reliability.

Modern traffic light systems employ various technologies, including timers, sensors, and microcontrollers, to manage traffic flow dynamically. Microcontrollers, like the Arduino used in this project, have become increasingly popular due to their affordability, ease of programming, and versatility. Studies have shown that Arduino-based traffic light systems can effectively manage traffic at intersections, providing a cost-effective solution for small-scale implementations (Naveen, 2017). These microcontrollers can be programmed to control the timing and sequence of traffic lights, adapting to traffic conditions and optimizing flow. The Arduino platform, introduced in 2005, has revolutionized the way enthusiasts and professionals approach electronics and programming projects. It provides an accessible entry point for designing and implementing a wide range of electronic applications. In a comparative study, it was found that Arduino-based traffic light systems are not only economical but also offer high reliability and ease of maintenance compared to traditional traffic light controllers (Srinivas and Sreenivasulu, 2018). The Arduino Uno, based on the ATmega328P microcontroller, offers digital and analog input/output pins, making it suitable for controlling various electronic devices, including LEDs used in traffic lights.

Implementing a two-lane traffic light model using Arduino serves as an excellent educational tool, allowing students and hobbyists to understand the principles of traffic management, electronics, and programming. Studies have demonstrated the feasibility of using Arduino for traffic control, with successful implementations in various configurations, including two-lane and four-way intersections (Kumar et al., 2019). It also provides a practical demonstration of how technology can be applied to solve real-world problems. The knowledge gained from such projects can be further expanded to develop more complex systems, such as smart traffic lights that respond to real-time traffic data.

### II. MATERIALS AND METHODS

This section provides a detailed overview of the components used and the procedures followed in the design and construction of the two-lane traffic light model. An outline of the materials employed, including electronic components, tools, and any additional resources utilized throughout the project is presented. The project is divided into four units, namely; power supply unit, control unit, traffic light unit and wiring and interconnection unit.

# a. Power Supply Unit

The Power Supply Unit (PSU) for the project is responsible for delivering stable and regulated power to the electronic components, ensuring their proper functioning. It consisted of a 12V power adapter and a voltage regulator (LM7805).

The 12V power adapter served as the primary power source, converting AC voltage from a standard power outlet into a stable DC voltage suitable for electronic devices. This adapter provides the necessary voltage to operate the entire system.

The LM7805 voltage regulator, a linear regulator, further refines the power supply by converting the 12V input voltage to a regulated 5V output. This regulation is vital for preventing voltage fluctuations that could disrupt the operation of sensitive electronics, such as the Arduino Uno and other components in the circuit.

The wiring was done by connecting the 12V power adapter to a standard AC power outlet. Its DC output was then directed to the input pin of the LM7805 voltage regulator. The regulated 5V output from the

LM7805 was connected to the appropriate power input pins, such as the 5V pin on the Arduino Uno and other electronic components.

Safety was considered when designing the Power Supply Unit. It is essential to ensure that the current rating of the power adapter meets the requirements of the circuit without exceeding its maximum capacity. Also, proper heat dissipation measures were taken, especially for the LM7805 voltage regulator, which may generate heat during operation. Adequate ventilation was provided to dissipate heat effectively and prevent overheating issues. The block diagram of regulated power supply unit is shown in Figure 1.

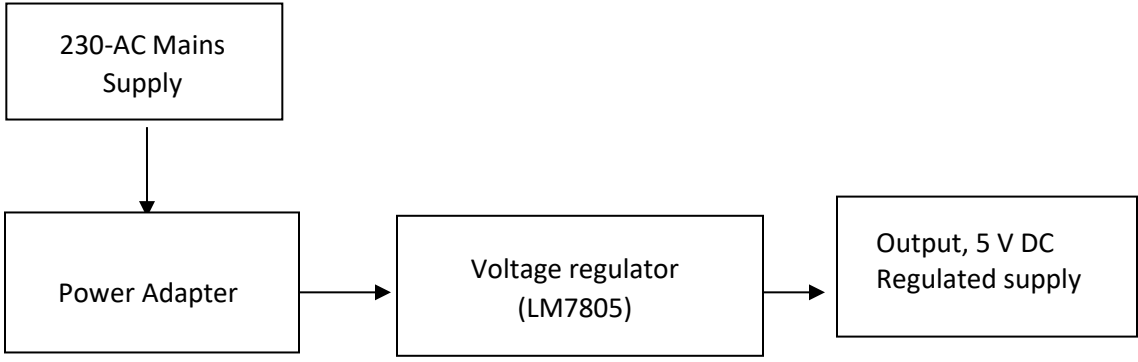


Figure 1: Block diagram of the regulated power supply unit

# b. Control Unit

The control unit was based on the Arduino Uno, a versatile and widely-used microcontroller platform. The Arduino Uno serves as the brain of the traffic light system, managing the timing sequences and transitions of the traffic lights. It was programmed to control the behaviour of the lights, ensuring that vehicles from the main road and the adjacent road were properly managed, preventing conflicts and ensuring smooth traffic flow.

The Arduino Uno is a microcontroller board based on the ATmega328P microcontroller. It features 14 digital input/output pins, 6 analog inputs, a 16 MHz quartz crystal, a USB connection, a power jack, an ICSP header, and a reset button. The digital pins were used to control the LEDs representing the traffic lights, while the analog pins can be used for sensors or other input devices if needed.

A USB programming cable was used to upload the code to the Arduino Uno. This cable connects the Arduino Uno to a computer, allowing the user to write and upload the program that dictates the traffic light sequences. The USB connection also provides power to the Arduino Uno during the programming process. The Arduino Integrated Development Environment (IDE) on the computer was used to write the code in a simplified version of C++, compile it, and upload it to the microcontroller. The USB cable is essential for this process, as it facilitates communication between the computer and the Arduino Uno, enabling the transfer of the control logic to the microcontroller. The front view of Arduino Uno that was used in the project is displayed in figure 2 while Table 1 shows the specifications of the same.



Figure 2: Front View of Arduino Uno

Table 1: Arduino Uno Specifications

Features	Specifications
Microcontroller	ATmega328P
Operating Voltage	5V
Input Voltage	7-12V
Input Voltage (limits)	6-20V
Digital I/O Pins	14 (of which 6 provide PWM output)
PWM Digital I/O Pins	6 (D3, D5, D6, D9, D10, D11)
Analog Input Pins	6 (A0-A5)
DC Current per I/O Pin	20 mA
Flash Memory	32 KB (ATmega328P)
SRAM	2 KB (ATmega328P)
EEPROM	1 KB (ATmega328P)
Clock Speed	16 MHz
LED (BUILTIN)	13

# c. Traffic Light Unit

The Traffic Light Unit is a crucial component of the two-lane traffic light model, responsible for visually signaling the traffic flow directions using LEDs. This unit consisted of two pairs of LEDs arranged to represent the standard red, yellow, and green lights used in real traffic signals. These LEDs were controlled by the Arduino Uno microcontroller, which dictates their ON/OFF states based on the programmed traffic light sequences. Each set of LEDs corresponds to a specific direction of traffic, ensuring that vehicles from the main road and the adjacent road were appropriately managed.

The LEDs in the Traffic Light Unit were divided into red, yellow, and green categories. Red LEDs indicate when vehicles must stop, yellow LEDs signal caution and prepare drivers for a change in the traffic signal, and green LEDs indicate when vehicles were allowed to proceed. Each traffic direction, both the main road

and the adjacent road, have its own set of these LEDs. This allows the traffic flow to be controlled independently for each direction, ensuring that vehicles from one road can proceed while those from the other road are stopped.

Current-limiting resistors were used in series with each LED to limit the current flowing through them, preventing damage due to excessive current. Typically, 220 ohms resistor was used for this purpose. These resistors ensured that the LEDs received the appropriate amount of current, prolonging their lifespan and maintaining consistent brightness.

The LEDs were connected to the digital output pins of the Arduino Uno, which controls them by sending high (5V) or low (0V) signals to the pins, turning the LEDs ON and OFF according to the traffic light sequence programmed in the Arduino. The typical sequence involves the green light turning ON to indicate that vehicles can proceed, followed by the green light turning OFF and the yellow light turning ON briefly to signal an upcoming stop. Finally, the yellow light turns OFF and the red light turns ON to indicate a stop. The red light then turns OFF, returning to the green light for the next cycle. This sequence can be adjusted in the Arduino code to match desired traffic flow patterns, such as longer green light durations for the main road and shorter ones for the adjacent road, or vice versa.

By using the Arduino Uno to control the LEDs, the Traffic Light Unit effectively simulates a real-world traffic light system, providing clear visual signals for vehicle movement along the main and adjacent roads. This setup allows for flexible and programmable control, enabling experimentation with different traffic light sequences and timings to optimize traffic flow and enhance safety.

# d. Wiring and Interconnection Unit

The wiring and interconnection unit is a vital part of the model that ensured all components were properly connected to facilitate smooth operation. This unit involves the careful routing of electrical connections between the Arduino Uno, LEDs, current-limiting resistors, power supply, and any other necessary components. Proper wiring ensures reliable communication between the controller and the traffic lights, allowing the system to function as intended.

The wiring of the Traffic Light Unit involved connecting each LED to a dedicated digital output pin on the Arduino Uno. The anode (positive leg) of each LED was connected to the digital pin via a current-limiting resistor, while the cathode (negative leg) was connected to the ground (GND) pin on the Arduino Uno. This setup ensures that each LED can be individually controlled by the Arduino, allowing for precise timing and coordination of the traffic signals.

The 12V power adapter was connected to the input of the LM7805 voltage regulator, which steps down the voltage to a stable 5V output suitable for powering the Arduino Uno and other components. The positive terminal of the power adapter was connected to the VIN pin of the LM7805, while the negative terminal was connected to the GND pin. The regulated 5V output from the LM7805 was then connected to the 5V and GND pins on the Arduino Uno, providing it with the necessary power to operate.

All these connections were typically made on a breadboard for prototyping purposes. Using a breadboard allows for easy adjustments and troubleshooting during the development phase. Once the connections are verified and the system operates correctly, the circuit can be transferred to a more permanent setup, such as soldering the components onto a vero board, ensuring durability and stability of the connections.

### e. Writing and Uploading of the Control Code

For the two-lane traffic light model project, the Arduino Integrated Development Environment (IDE) was used to write and upload the control code to the Arduino Uno, managing the traffic light sequences and timings. The following was the code written in Arduino IDE and uploaded to the Arduino Uno to manage the sequence and timing of the traffic light:

```
// Define the pins for the traffic lights
const int redLight1 = 2;
const int yellowLight1 = 3;
const int greenLight1 = 4;
const int redLight2 = 5;
const int yellowLight2 = 6;
const int greenLight2 = 7;
void setup() {
// Set the traffic light pins as outputs
pinMode(redLight1, OUTPUT);
 pinMode(yellowLight1, OUTPUT);
 pinMode(greenLight1, OUTPUT);
 pinMode(redLight2, OUTPUT);
pinMode(yellowLight2, OUTPUT);
 pinMode(greenLight2, OUTPUT);
void loop() {
// Main road green, adjacent road red
 digitalWrite(greenLight1, HIGH);
 digitalWrite(redLight2, HIGH);
 delay(15000); // Green light for main road for 15 seconds (15 seconds)
 // Main road yellow
 digitalWrite(greenLight1, LOW);
 digitalWrite(yellowLight1, HIGH);
 delay(6000); // Yellow light for main road for 6 seconds (6 seconds)
 // Main road red, adjacent road green
 digitalWrite(yellowLight1, LOW);
 digitalWrite(redLight1, HIGH);
 digitalWrite(redLight2, LOW);
 digitalWrite(greenLight2, HIGH);
 delay(15000); // Green light for adjacent road for 15 seconds (15 seconds)
 // Adjacent road yellow
 digitalWrite(greenLight2, LOW);
 digitalWrite(yellowLight2, HIGH);
 delay(6000); // Yellow light for adjacent road for 6 seconds (6 seconds)
```

```
// Reset to initial state digitalWrite(yellowLight2, LOW); digitalWrite(redLight1, LOW); digitalWrite(redLight2, HIGH); delay(3000); // Small delay before restarting the loop (3 second) }
```

# III. Results and Testing

The design and construction of the two-lane traffic light successfully demonstrated the functionality and effectiveness of the proposed system. The project was divided into four main units: Power Supply Unit, Control Unit, Traffic Light Unit, and Wiring and Interconnection Unit. Each unit played a critical role in ensuring the proper operation of the traffic light model.

The Power Supply Unit was effective in providing stable and regulated power to the entire system. The 12V power adapter efficiently converted AC voltage to DC voltage, which was then further refined by the LM7805 voltage regulator to a stable 5V output. This ensured that all electronic components, particularly the Arduino Uno, received consistent and reliable power, preventing any operational disruptions caused by voltage fluctuations. Safety measures, including adequate heat dissipation, were implemented to ensure the longevity and reliability of the power supply.

The Control Unit, based on the Arduino Uno microcontroller, successfully managed the timing sequences and transitions of the traffic lights. The Arduino Uno was programmed using the Arduino Integrated Development Environment (IDE) to control the LEDs representing the traffic lights. The uploaded code dictated the behaviour of the lights, ensuring a smooth and conflict-free flow of traffic. The control logic was effectively transferred to the Arduino via a USB programming cable, facilitating easy updates and modifications to the traffic light sequences.

The Traffic Light Unit comprised two sets of LEDs arranged to represent the red, yellow, and green lights used in standard traffic signals. Each set of LEDs was connected to the digital output pins of the Arduino Uno and controlled based on the programmed traffic sequences. Current-limiting resistors were used in series with each LED to prevent damage due to excessive current. The LEDs provided clear and bright visual signals, effectively simulating a real-world traffic light system. The sequences were programmed to manage the flow of vehicles from both the main road and the adjacent road, ensuring proper traffic management and safety.

The Wiring and Interconnection Unit ensured all components were correctly connected, allowing smooth communication between the control unit and the traffic lights. The connections were made on a breadboard for prototyping, providing flexibility for adjustments and troubleshooting. Once the wiring was verified, the circuit could be transferred to a more permanent setup for increased durability. The careful routing of electrical connections facilitated reliable operation, with each LED being individually controlled by the Arduino.

The model was tested and observed to function correctly, with the LEDs switching according to the programmed sequence. The main road's traffic lights and the adjacent road's traffic lights operated independently but in a coordinated manner, preventing traffic conflicts. The visual signals were clear and bright, making it easy to interpret the traffic instructions. Figure 3 is the layout of the two-lane traffic light system, while Figures 4 and 5 depict a prototype setup of the traffic light control circuit.

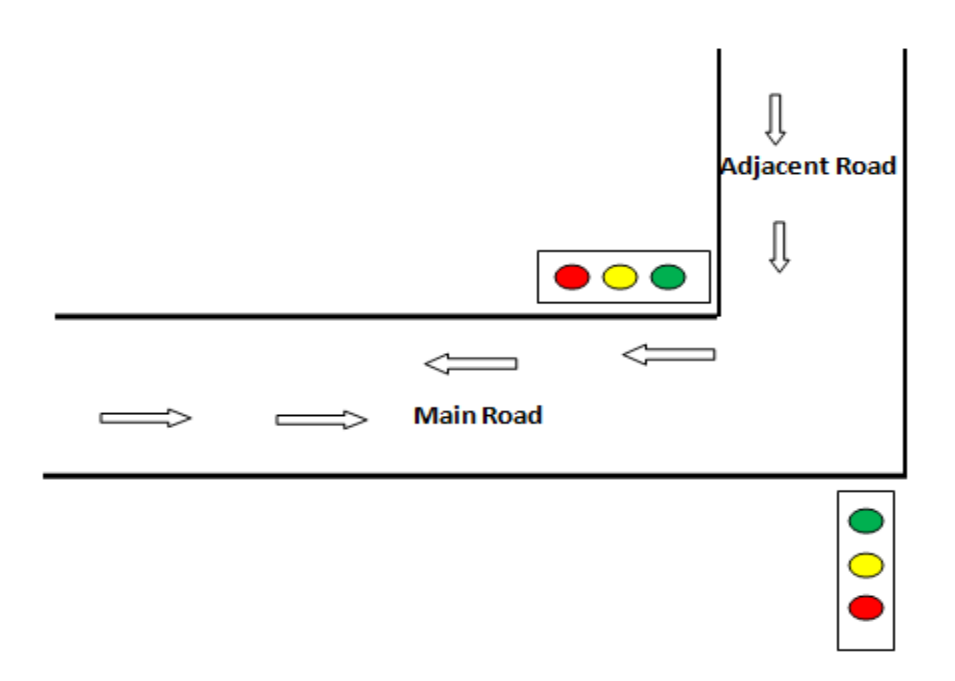


Figure 3: Layout of the Two-Lane Traffic Light System

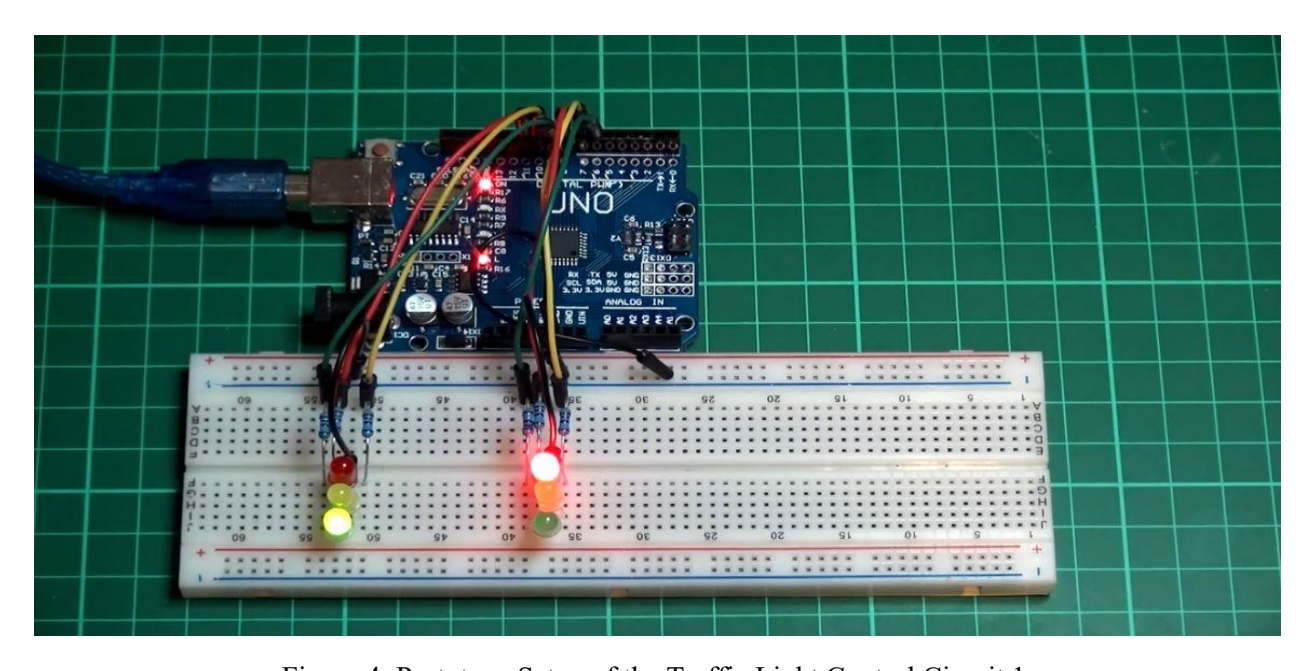


Figure 4: Prototype Setup of the Traffic Light Control Circuit 1

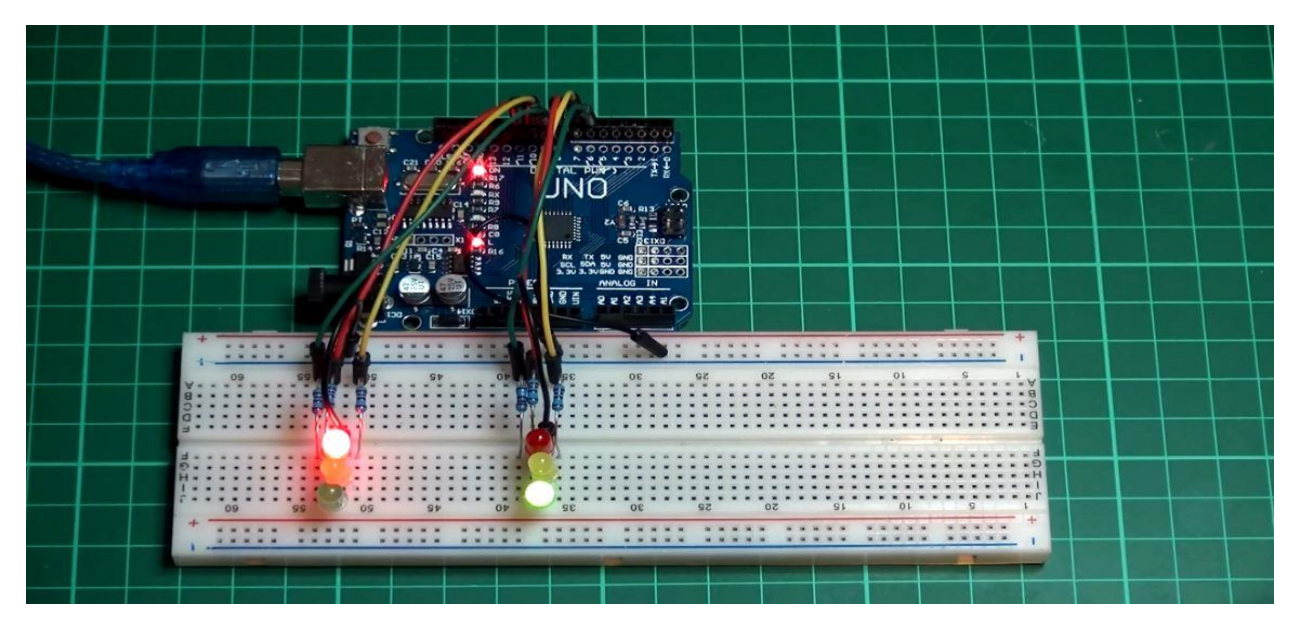


Figure 5: Prototype Setup of the Traffic Light Control Circuit 2

# IV. Discussion

The project showcases a practical and efficient approach to traffic management using modern microcontroller technology. The success of this project can be attributed to the careful selection and integration of components, systematic design, and effective programming. Each unit of the project contributed significantly to the overall functionality, ensuring smooth and reliable operation.

In the loop function, the traffic light sequence begins with the green light for the main road and the red light for the adjacent road being turned ON. This state remains for 15 seconds, allowing vehicles on the main road to proceed while vehicles on the adjacent road must stop. Following this, the main road's green light turns OFF and the yellow light turns ON for 6 seconds, signaling drivers to prepare to stop.

After the yellow light phase for the main road, the red light for the main road and the green light for the adjacent road are activated. This state also lasts for 15 seconds, permitting vehicles from the adjacent road to pass while those on the main road must stop. Subsequently, the green light for the adjacent road turns OFF, and the yellow light is activated for 6 seconds, warning drivers to prepare to stop.

Finally, the code resets the lights to the initial state: the yellow light for the adjacent road is turned OFF, and the red lights for both roads are set, with a brief delay of 3 seconds before the loop restarts. This delay ensures a smooth transition back to the main road being green and the adjacent road being red. The continuous cycling of these phases effectively simulates a real-world traffic control system, managing the flow of vehicles and ensuring orderly transitions between traffic states.

# V. Conclusion

The development and implementation of a two-lane traffic light control system using Arduino has been successfully achieved. This project demonstrates the practical application of microcontroller programming to manage traffic flow efficiently. The use of LEDs to simulate real-world traffic lights, controlled by an Arduino Uno, has provided a clear and functional model of a traffic management system. The system's ability to alternate traffic signals between the main road and adjacent road, with appropriate timing intervals for red, yellow, and green lights, ensures an organized and safe traffic flow. This project not only

underscores the importance of traffic light systems in urban planning but also showcases the potential of using simple electronic components and microcontrollers for educational and prototyping purposes. Future enhancement could be incorporating real-time traffic data using sensors to dynamically adjust the traffic light sequences based on actual traffic conditions. This could further optimize traffic flow and reduce congestion.

# Acknowledgement

The author sincerely thanks the management of NICTM and TETFUND for their invaluable support and funding, which made this project feasible.

#### Reference

Bilal, G., & Khaled, E. (2016). Smart Traffic Light Control System. Conference Paper.

Dinesh, R. & Swapnil, K. (2012). Intelligent Traffic Signal Control System Using Embedded System". G.H Raisoni College of Engineering, Nagpur. Innovative Systems Design and Engineering.

Kumar, S., Singh, R., & Verma, P. (2019). "Design and Implementation of Traffic Light Control System Using Arduino." International Journal of Engineering Research & Technology, Vol. 8, Issue 7, pp 1-6.

Malik T., Ti, S. & Hongchi, S. (2007). Adaptive Traffic Light Control with Wireless Sensor Networks. Article

Nang H. & Chaw M. N. (2014). Impletation of Modern Traffic Light Control System. Department of Electronic Engineering, Mandalay Technological University, Myanmar. International Journal of Scientific and Research Publications.

Naveen, P. (2017). "Arduino Based Traffic Light Control System." International Journal of Scientific and Research Publications, Vol. 7, Issue 12, pp 250-254.

Parkhi, M. A.A., Peshattiwar, A.A. & Pande, K.G. (2016). Intelligent Traffic System Using Vehicle Density". Yeshwantrao Chavan College of Engg., Nagpur. International Journal of Electrical and Electronic Engoneers.

Rao, N. (2019). Design and development of automatic traffic light control system. International Journal of Innovative Research in Electrical, Electronics, Instrumentation and Control Engineering, Vol. 7, Issue 6, pp. 55 - 57.

Srinivas, K., & Sreenivasulu, P. (2018). "Comparative Study of Traffic Light Control Systems." International Journal of Advanced Research in Electrical, Electronics and Instrumentation Engineering, Vol. 7, Issue 6, pp. 3565-3571.

Tolulope, O., & Patrick, O. (2014). Design and implementation of a four-way junction prototype crossroad traffic light control system. Journal of Advancement in Engineering and Technology. Pp 1-9

Uzondu, C., Jamson, S & Lai, F. Exploratory study involving observation of traffic behaviour and conflicts in Nigeria using the Traffic Conflict Technique," Safety Science, vol. 110, pp. 273-284

# The Design and Implementation of an Electronic Sign Pattern Display

Engr. Clement Agbeboaye

Department of Electrical/Electronic Engineering Technology, National Institute of Construction Technology and Management, Uromi, Edo State, Nigeria.

c.agbeboaye@nict.edu.ng

#### **Abstract**

This project presents the design and implementation of an electronic sign pattern display utilizing a 48x8 LED matrix, Arduino Nano microcontroller, and SN74HC595N shift registers. The primary objective was to develop a scalable, efficient, and reliable display system capable of presenting dynamic, scrolling messages. The hardware design incorporated BD139 transistors for current amplification, ensuring the microcontroller and shift registers operated within safe limits. A 12V power adapter and LM7805 voltage regulator provided stable 5V power, with filtering capacitors ensuring clean voltage supply. The plywood housing offered robust protection and adequate ventilation for the components. The control code, written in C++, leveraged the Arduino IDE and LedControl library to manage data transmission and display control efficiently. The system was tested extensively, verifying the functionality of the LED matrix, the smoothness of the scrolling message, and the stability of the power supply. The message "Welcome to the Department of Electrical and Electronic Engineering Technology, NICTM, Uromi" was successfully displayed with high clarity and uniform brightness. This project demonstrates the practical application of integrating microcontrollers and peripheral components to create dynamic electronic displays. The results validate the design and implementation strategies, highlighting the potential for future enhancements such as interactive features and larger display configurations. This work provides a foundation for further innovation in electronic signage, emphasizing the importance of interdisciplinary approaches in developing advanced visual communication tools. The successful outcome not only meets the project's initial goals but also inspires continued exploration and development in electronic display technologies.

Keywords: Electronic Display, Arduino nano, LED Matrix, Shift Register, Scrolling Message

#### I. Introduction

The evolution of display technologies has revolutionized communication and information dissemination across various sectors, from public signage to digital advertising. Electronic sign pattern displays, in particular, have become an integral part of modern visual communication due to their ability to present dynamic and engaging content. Electronic sign pattern displays, leveraging Light Emitting Diodes (LEDs) and advanced microcontroller systems, represent a significant advancement in visual communication capabilities (Smith, 2018).

The history of electronic displays dates back to the early 20th century with the invention of cathode-ray tubes (CRTs) used primarily in television sets and computer monitors. The subsequent development of liquid crystal displays (LCDs) and light-emitting diodes (LEDs) marked significant milestones in the evolution of display technologies. LEDs, introduced in the 1960s, initially served as simple indicator lights but have since evolved into versatile components for complex display systems due to their low power consumption, long lifespan, and vibrant color output (Smith, 2018). Due to its clear bright light, way of displaying such as rolling left, right or fancy appearances, it has gained popularity around the world (Sheeba et al., 2018; Dwik et al., 2020).

The evolution of LED displays has been driven by continuous advancements in semiconductor technology and microelectronics. Modern LED displays can be found in a wide range of applications, from small handheld devices to large outdoor billboards and are used for different purposes. In banks, it is used to display interest rates as well as exchange rates, in hotels and pubs; it is used to display menu and prices (Obiechine et al., 2013; Aribisala et al., 2018). The arrangement of LEDs in matrix configurations, controlled by microcontrollers like the Arduino Nano and interfaced with shift registers such as the SN74HC595N, enables the creation of versatile and dynamic display patterns capable of showcasing text, graphics, and animations (Brown, 2019).

Microcontrollers play a pivotal role in controlling LED matrices by managing individual LEDs through shift registers. The Arduino Nano, for instance, is widely used for its compact size, ease of programming, and compatibility with shift register ICs such as the SN74HC595N. Research by Brown (2019) emphasizes the importance of efficient hardware-software integration to optimize display performance and functionality.

Despite the significant advancements in electronic display technologies, several challenges remain in the design and implementation of efficient and scalable electronic sign pattern displays. Traditional display systems often suffer from limitations such as high power consumption, complex wiring, and inadequate control over individual display elements. These issues hinder the performance and scalability of electronic displays, particularly in applications requiring dynamic content and high resolution. According to Taylor (2021), while existing literature has explored various aspects of LED matrix displays and microcontroller applications, gaps persist regarding comprehensive methodologies for maximizing display functionality and user engagement. This study aims to address these gaps by proposing a systematic approach that integrates insights from the domains of electrical engineering, computer science, and human-computer interaction into the design.

# **II.** Definition of Terms

#### a. Microcontroller

A microcontroller is a compact integrated circuit designed to execute specific tasks in embedded systems. It contains a CPU, memory (both volatile RAM and non-volatile ROM or Flash), and various I/O peripherals all on a single chip. Microcontrollers are commonly used in electronic devices for control and automation purposes due to their low power consumption and cost-effectiveness.

#### b. Shift Register

A shift register is an integrated circuit that stores and shifts data serially (bit by bit) in response to clock pulses. It typically consists of a chain of flip-flops where each flip-flop stores one bit of data. Shift registers are used to expand the number of outputs from a microcontroller or other digital device, allowing control of multiple outputs (such as LEDs) with fewer pins.

# c. LED Matrix

An LED matrix is a grid of Light Emitting Diodes (LEDs) arranged in rows and columns. Each LED can be individually controlled to display alphanumeric characters, symbols, or simple graphics. LED matrices are commonly used for displaying information in electronic devices where a visual output is required.

### d. Transistor

A transistor is a semiconductor device used to amplify or switch electronic signals and electrical power. It consists of three terminals: the emitter, the base, and the collector. Transistors are fundamental building blocks in electronic circuits, used for tasks such as amplification, switching, and signal modulation.

#### e. Resistors

Resistors are passive electronic components that limit or control the flow of electric current in a circuit. They are characterized by their resistance value, measured in ohms ( $\Omega$ ). Resistors are used to adjust signal levels, bias active elements like transistors, terminate transmission lines, and divide voltages.

Figure 1 is the block diagram of the Electronic Sign Pattern Display System.

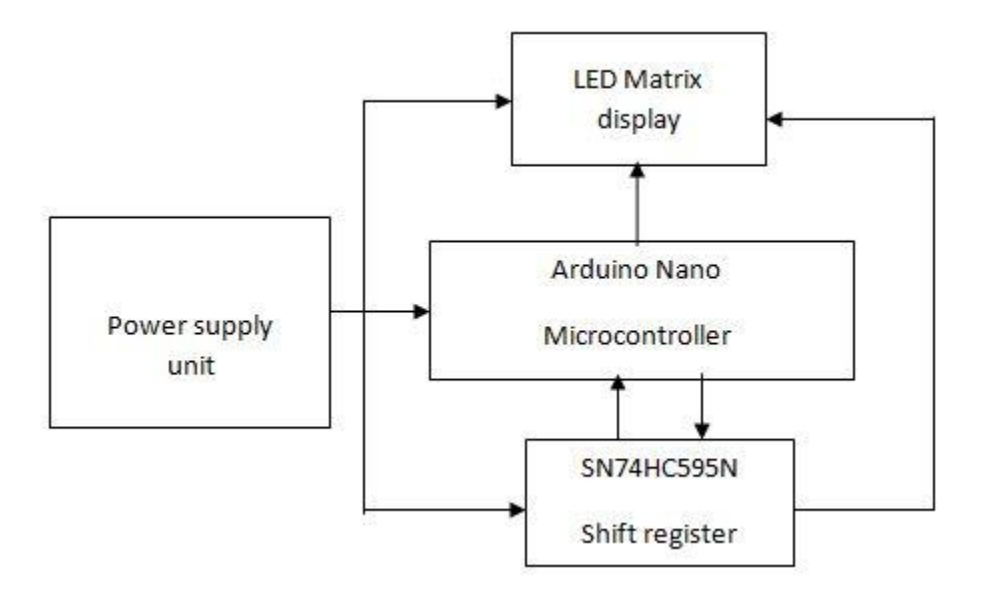


Figure 1: Block diagram of the Electronic Sign Pattern Display System

### III. Materials and Methods

This section provides a detailed overview of the components used and the procedures followed in the design and implementation of the project. An outline of the materials that were utilized, including electronic components, tools, and any additional resources employed throughout the project is presented. The project is divided into four units, namely; LED Matrix unit, control unit, power supply unit and housing and mechanical unit.

#### a. LED Matrix Unit

The LED Matrix Unit forms the core display component of the electronic sign pattern display project, consisting of 384 LEDs arranged in a 48x8 grid. This unit was meticulously assembled with all the negative terminals (cathodes) of the LEDs in each row soldered together, and all the positive terminals (anodes) in each column similarly soldered together. This configuration allows for precise control of individual LEDs within the matrix, facilitating the creation of dynamic patterns and text displays.

To interface the LED matrix with the control circuitry, six connectors, each containing 8 wires was used to link every set of 8 columns to a separate SN74HC595N shift register. This setup ensures efficient and organized data transfer from the microcontroller to the LED columns. Additionally, a seventh connector was employed to connect the 8 rows to another shift register in the Arduino Nano circuit, completing the control network. This arrangement allows the Arduino Nano, in conjunction with the shift registers, to selectively activate specific LEDs by coordinating signals sent to the appropriate rows and columns, thus enabling the desired visual output on the LED matrix. Figure 2 and 3 present the front and back view of the LED matrix display.



Figure 2: LED Matrix Display – Front View



Figure 3: LED Matrix Display – Back View

#### b. Control Unit

The Control Unit is the pivotal component of the electronic sign pattern display, coordinating the integration of the microcontroller with the LED matrix to achieve the desired visual effects. Central to this unit is the Arduino Nano microcontroller, which was mounted on a dedicated printed circuit board (PCB) alongside a single SN74HC595N shift register. This primary PCB also incorporates

eight BD139 transistors, which are essential for amplifying the current to drive the LEDs efficiently, thus ensuring that the microcontroller and shift registers were not subjected to excessive load.

To manage the extensive 48x8 LED matrix, additional control circuitry was distributed across two supplementary PCBs, each hosting three SN74HC595N shift registers. These PCBs facilitate the division of control signals, with each shift register on these boards responsible for regulating 8 columns of the matrix. The row connector wire from the LED matrix was directly linked to the shift register on the Arduino Nano PCB, enabling the microcontroller to selectively activate specific rows. Concurrently, the six column connector wires were connected to the shift registers on the other two PCBs, ensuring comprehensive control over all 48 columns.

For optimal current regulation and signal stability, each shift register was paired with eight 330-ohm resistors to limit the current flow and protect the components. The utilization of a female header ensures secure and efficient interfacing between the LED matrix and the shift registers. Additionally, eight 8K ohm resistors were incorporated for the shift register interfaced with the row LED connector to enhance signal integrity. This carefully engineered configuration of the Control Unit ensures precise and reliable manipulation of the LED matrix, facilitating the creation of complex patterns and smooth scrolling text displays. Figure 4 presents the fabricated control circuit.

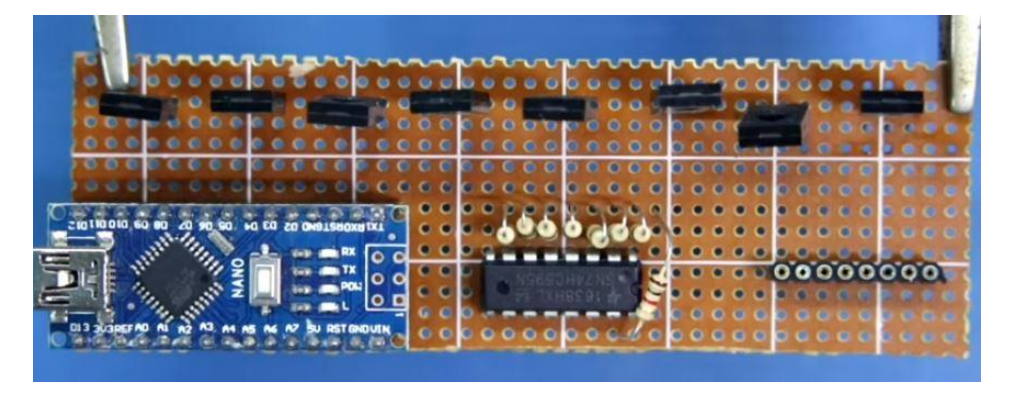


Figure 4: Fabricated Control Circuit

#### c. Power Supply Unit

The Power Supply Unit of the electronic sign pattern display is crucial for providing stable and sufficient power to all components. The unit utilizes a 12V power adapter as the primary power source, which was then regulated down to 5V using an LM7805 voltage regulator. This setup ensures that the Arduino Nano, shift registers, BD139 transistors, and LED matrix receive the required 5V for efficient operation. The choice of a 12V adapter is practical due to its ability to supply adequate current for the entire display system.

The LM7805 voltage regulator plays a key role in maintaining a steady 5V output from the 12V input, protecting sensitive electronic components from voltage fluctuations. Filtering capacitors were employed at both the input and output of the regulator to smooth out voltage ripples and transient spikes, ensuring a clean and stable voltage supply. This is essential for the reliable operation of the microcontroller and the control circuitry.

Additionally, the power supply unit includes protection mechanisms such as fuses for overcurrent protection and diodes for reverse polarity protection. Power was distributed efficiently from the regulator to all components via adequately gauged wiring and connectors. Current-limiting resistors were used with the LED matrix to prevent overdriving the LEDs, ensuring uniform brightness and protecting the LEDs from damage.

# d. Housing and Mechanical Unit

The Housing and Mechanical Unit was constructed using plywood, providing a sturdy and cost-effective enclosure for all the components of the electronic sign pattern display. This unit securely housed the LED matrix, PCBs, Arduino Nano, shift registers, BD139 transistors, and power supply components, ensuring they were protected and well-supported. The plywood enclosure was designed to withstand environmental factors and mechanical stress while maintaining a lightweight profile. Ventilation slots were incorporated to facilitate efficient heat dissipation, preventing overheating of the electronic components. The design included accessible ports and connectors, allowing for easy interfacing, troubleshooting, and future upgrades. The plywood construction ensured that the LEDs were properly aligned, offering a clear and visually appealing display while protecting the internal circuitry from dust, moisture, and accidental damage.

# e. Writing and Uploading of the Control Code

The writing and uploading of the control code is a critical phase in the implementation of the electronic sign pattern display, enabling the hardware components to function cohesively to produce the desired visual outputs. The process begins with developing the code in the Arduino Integrated Development Environment (IDE), a user-friendly platform that supports writing, compiling, and uploading code to the Arduino Nano microcontroller. The control code was written in C++ and leverages various libraries, such as the LedControl library, which simplifies the interaction with the SN74HC595N shift registers and the LED matrix. The code includes functions to initialize the hardware, control individual LEDs, and manage the display patterns. Key features such as scrolling text and dynamic updates were programmed to ensure the display meets the required specifications. The code was structured to handle the serial-to-parallel data conversion efficiently, ensuring smooth and flicker-free operation of the LED matrix. Once the code was written and thoroughly tested in the Arduino IDE through simulations and debugging, it was uploaded to the Arduino Nano via a USB connection. The IDE provides a straightforward interface for selecting the appropriate board and port, compiling the code, and transferring it to the microcontroller. After uploading, the Arduino Nano executes the control code, driving the shift registers and transistors to illuminate the LED matrix as per the programmed instructions. This process enables the creation of intricate patterns and messages on the display, fulfilling the project's functional requirements. The following was the code written in Arduino IDE and uploaded to the Arduino nano to display the scrolling message "Welcome to the Department of Electrical and Electronic Engineering Technology, NICTM, Uromi":

```
// Pin connections for the LedControl const int dataInPin = 2; // Pin connected to DS (Data) on the first shift register const int clkPin = 3; // Pin connected to SH_CP (Clock) const int loadPin = 4; // Pin connected to ST_CP (Latch) const int numDevices = 6; // Number of 8x8 matrices
```

LedControl lc = LedControl(dataInPin, clkPin, loadPin, numDevices);

const char\* message = "Welcome to the Department of Electrical and Electronic Engineering Technology, NICTM, Uromi";

```
// Define a font array to map characters to LED patterns (8x8 bitmaps)
byte font[96][8] = {
 // Add 8x8 bitmaps for characters ' 'to '~' here
 // Example for 'A':
  B00011000,
  B00100100,
  B01000010,
  B01000010,
  B01111110,
  B01000010,
  B01000010,
  B01000010
 // Add other characters as needed
};
void setup() {
 // Initialize the LedControl library
 for (int i = 0; i < numDevices; i++) {
  lc.shutdown(i, false);
                            // Wake up displays
  lc.setIntensity(i, 8); // Set brightness level (0 is min, 15 is max)
                          // Clear display register
  lc.clearDisplay(i);
void loop() {
 scrollMessage(message);
void scrollMessage(const char* msg) {
 int len = strlen(msg);
 for (int charIndex = 0; charIndex < len; charIndex++) {
  char c = msg[charIndex];
  if (c < 32 \parallel c > 127) continue; // Skip non-printable characters
  byte charBitmap[8];
  memcpy(charBitmap, font[c - 32], 8); // Fetch the character's bitmap
  for (int col = 0; col < 8; col++) {
   for (int row = 0; row < 8; row++) {
    int bit = (charBitmap[row] >> col) \& 0x01;
    lc.setLed((charIndex * 8 + col) / 8, col % 8, row, bit);
```

```
}
delay(100);
lc.clearDisplay((charIndex * 8 + col) / 8); // Clear display after scrolling a column
}
}
}
```

# IV. Results and Testing

The results and testing phase of the electronic sign pattern display project focused on evaluating the functionality, performance, and reliability of the system. Upon assembling the hardware and uploading the control code, initial tests were conducted to verify the basic operation of the LED matrix. Each segment of the 48x8 LED matrix was illuminated sequentially to ensure all LEDs were properly connected and functioning. This initial verification confirmed that the soldering and wiring were correctly implemented and that the LEDs responded appropriately to control signals from the Arduino Nano and SN74HC595N shift registers. Figure 5 presents the complete fabricated circuit for the project.

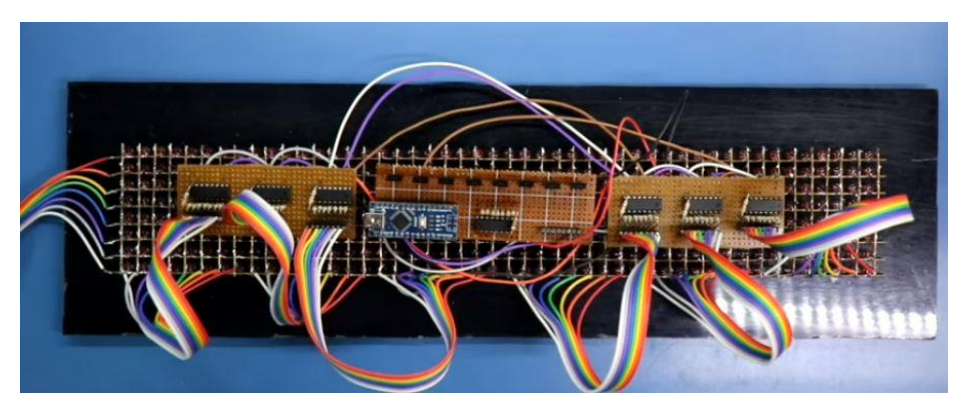


Figure 5: Complete fabricated circuit for Electronic Sign Pattern Display System

Subsequent tests involved the scrolling display of the message "Welcome to the Department of Electrical and Electronic Engineering Technology, NICTM, Uromi." The control code was designed to shift each character smoothly across the LED matrix. The primary focus during these tests was to check for uniform brightness across the LEDs, the clarity of the displayed characters, and the smoothness of the scrolling effect. The message successfully scrolled from right to left, with each character distinctly visible and well-formed, indicating that the integration of hardware and software components was successful. Figure 6 presents the scrolling message display.



Figure 6: Scrolling Message Display.

The performance testing also included evaluating the power consumption and thermal management of the system. Using a 12V power adapter and the LM7805 voltage regulator, the system maintained a stable 5V output without significant voltage drops or overheating. The inclusion of filtering capacitors ensured a clean power supply, free of ripples and transient spikes, which is critical for the stable operation of the microcontroller and LED matrix. The ventilation slots in the plywood housing facilitated adequate heat dissipation, preventing any thermal issues during prolonged operation.

Reliability tests were conducted by running the display continuously over extended periods to identify any potential issues such as flickering, dimming, or failure of individual LEDs. The display performed consistently, demonstrating robust construction and reliable operation. User feedback was also gathered to assess the readability and visual appeal of the scrolling message. The feedback indicated that the display was easily readable from various angles and distances, and the scrolling speed was appropriate for comfortable viewing.

# V. Discussion

The project successfully demonstrates the feasibility and effectiveness of using LEDs, microcontrollers, and shift registers to create a dynamic and engaging visual communication tool. The primary objective was to develop a scalable and efficient display capable of presenting moving messages with high clarity and reliability. The results from the testing phase indicate that this objective was met, highlighting several key points for discussion. One of the most significant achievements of the project was the seamless integration of the Arduino Nano microcontroller with the SN74HC595N shift registers and the BD139 transistors. This integration allowed for efficient control of the 48x8 LED matrix with minimal I/O pin usage on the microcontroller, thus simplifying the circuit design. The use of shift registers to expand the output capabilities of the Arduino Nano proved to be an effective strategy, enabling the precise control necessary for displaying detailed and smooth scrolling text. This demonstrates the viability of combining these components in similar future projects requiring extensive output control.

The decision to use a 12V power adapter in conjunction with the LM7805 voltage regulator ensured a stable 5V supply to the system. This configuration was critical for the reliable operation of the microcontroller and LEDs, as it provided consistent voltage regulation and minimized potential issues related to power fluctuations. The inclusion of filtering capacitors further enhanced the stability of the power supply, contributing to the overall reliability of the display. These design choices underscore the importance of robust power management in electronic display systems. The construction of the housing and mechanical unit using plywood was both cost-effective and practical. The plywood enclosure provided sufficient protection for the internal components while allowing for adequate ventilation and heat dissipation. This prevented overheating and ensured the longevity of the display during continuous operation. Additionally, the accessibility of ports and connectors facilitated easy maintenance and future upgrades, reflecting thoughtful design considerations aimed at enhancing user experience and system durability.

While the project achieved its primary goals, there are areas for potential improvement and further exploration. One such area is the optimization of the control code for greater efficiency and enhanced features. For example, incorporating more advanced animations and interactive capabilities could make the display more versatile. Additionally, exploring alternative materials for

the housing could offer improvements in durability and aesthetics, particularly for outdoor or harsh environments. Another aspect worth exploring is the scalability of the system. While the current project focused on a 48x8 LED matrix, scaling up the design to larger displays could present new challenges and opportunities. Investigating the use of more powerful microcontrollers or dedicated LED driver ICs could help manage larger matrices more effectively, opening the door to more extensive applications in digital signage and public information systems.

#### VI. Conclusion

The completion of the project marks a significant milestone in the practical application of electronic display technologies. This project not only showcases the ability to construct a functional LED matrix display but also highlights the potential for further innovation in the field. Through meticulous design, thoughtful component selection, and careful assembly, a robust system was created that demonstrates the capability of modern microcontrollers and peripheral components to deliver dynamic visual communication solutions. This project underscores the importance of interdisciplinary collaboration, blending principles from electrical engineering, computer science, and user interface design to achieve a cohesive and effective outcome. The successful integration of hardware and software components illustrates the critical role that comprehensive planning and testing play in the development of complex electronic systems. Moreover, the project provides a valuable case study for the educational and practical applications of electronic sign displays, serving as a model for similar initiatives.

Looking ahead, the findings and methodologies established in this project pave the way for future advancements in electronic signage. The adaptability of the design allows for enhancements in functionality, such as interactive features and more sophisticated display patterns. Additionally, the scalable nature of the LED matrix design opens up possibilities for larger and more intricate display systems, which could be employed in a variety of settings, from public information displays to commercial advertising.

# Acknowledgement

The author extends heartfelt gratitude to the management of NICTM and TETFUND for their invaluable support and funding, which enabled the successful completion of this project.

#### Reference

Aribisala, A., Martins, O., Otenaike, A., & Ajayi, J. (2018). Design and implementation of a sequential digital display for a Nigerian university. FUOYE Journal of Engineering and Technology, 3(2), 45-49.

Brown, P. (2019). LED technology in signage: A comprehensive overview. Journal of Display Technology, 15(3), 112-125.

Dwik, S., Amaya, M., & Somasundaram, N. (2020). Design and implementation of an RGB LED matrix display for embedded applications. International Journal of Innovative Technology and Exploring Engineering (IJITEE), 9(3), 2337-2343.

Obiechine, O., Don, O. and Uche.V, (2013). Design and construction of a dot matrix information display for the office of the vice chancellor, Pelegia Research Library, 4(1), 515 522.

Smith, J. (2018). Principles of LED display technology. Springer.

Sheeba, P. T., Aarthi M.J., Deepika.P, Sagaya Mary.B, (2018). "SMART ALERT LED DISPLAYSYSTEM USING IOT", International Journal of Science, Engineering and Technology Research (IJSETR) 7(4) 238-242.

Taylor, M. (2021). Applications of LED matrix displays in public information systems. Journal of Information Display, 22(4), 301-315.

# Computation of Amplification Factor of the Mechanical Power Amplifier for Different Rope Materials

Engr. Okojie, Godwin<sup>1</sup>; Engr. Agbonkhese Ason Kingsley<sup>2</sup>; Agbadua udukhomoshi Timothy

1,2,3 E- Mail: <u>g.okojie@nict.edu.ng</u>; <u>k.agbonkhese@nict.edu.ng</u>; u.timothy@nict.edu.ng

<sup>1,2,3</sup>Department of Mechanical Engineering Technology National Institute of Construction Technology and Management, Uromi, Edo State, Nigeria

#### **Abstract**

Engineering applications often must control a substantial output load using a relatively low control force. Mechanical power amplifiers come into play to address this requirement, providing rapid response and efficient power transfer. In this study, we focus on computing the amplification factor of a mechanical power amplifier for various rope materials, including leather, woven cotton, and steel. The experimental analysis involves a capstan mechanism, where a rope is wound around a motor-driven drum. The drum continuously rotates, but torque transmission occurs only when the input shaft constricts the drum. Our investigation aims to determine the amplification factor for different rope

types. The results reveal that leather contact is optimal when the number of turns is approximately two, yielding an amplification factor of 2.23. Woven cotton contact achieves an amplification factor of 1.867. while steel contact provides an amplification factor of 1.32. Interestingly, leather outperforms woven cotton and steel in terms of power amplification. These findings align well with experimental measurements and demonstrate the mechanical power amplifier's favorable performance.

Keywords: computation factor, mechanical power amplifier, capstan, rope materials

#### Introduction

The amplification factor of an optical amplifier is the factor that amplifies the input power. The performance of laser amplifiers is influenced by factors such as the characteristics of the laser gain medium, its excitation level, optical wavelength, and beam polarization. The length of the nonlinear crystal, pump intensity, beam diameters, and various other parameters influence the performance of optical parametric amplifiers. An electrical amplifier specifically made to boost the power of a signal fed into it is called a power amplifier (Bienert et al., 2022; Choi, 2023; Jeong et al., 2023; Wang et al., 2022). The input signal is amplified to a degree where it can power several output devices. Depending on their changes to the incoming signal, amplifiers can be categorized as current, voltage, or power amplifiers. In this paper, power amplifiers are examined from the perspective of mechanics. Mechanical power amplifiers are electronic devices that are built on the Capstan architecture. These amplifiers aim to increase the strength of an electrical signal. Utilizing motorized drum slides to pick up the slack on the free end of the rope, the capstan is a basic mechanical amplifier. The capstan is employed when the user is required to lift or pull anything heavier than they can handle. The twist count and coefficient of friction of the rope determine how much force is required on the free end to lift the load. By employing bands coupled to an input shaft and arm, the power amplifier may offer an output in both directions and accurate angular positioning (Thokale, 2016).

A mechanical device called a capstan mechanical amplifier is characterized by a drum and gear configuration and a single electrical motor powered by electrical energy. In most cases, capstans are utilized for lifting or pulling big objects with the assistance of winches. According to Starkey and Williams (2011), a capstan can dynamically magnify the input by altering the strain that is placed on the cable based on the input. These devices enhance the power share partially supplied to the drum and change its control force. Power can be provided in both directions between the input and output shafts by mounting two rotating drums in a back-to-back configuration (Gawande, 2018). Conventional electrical, hydraulic, and pneumatic transducers can all be replaced by this revolutionary device. Because of this, the chance of cumulative inaccuracy brought about by using transducers is reduced. When a flexible rope line is looped around a cylinder, the Capstan principle establishes a relationship between the holding force and the load force (Baser & Ilhan Konukseven, 2010; Li et al., 2022; Qi et al., 2018; Schumann et al., 2022). The friction between the rope and the drum is caused by applying force in the direction of rotation. The force exerted by the user will be amplified due to the generated friction, which will act in the same direction as the pull.

In a general sense, the goal of the capstan is to produce a suitable amount of friction force between the drum and the rope to allow the rope to travel at the same pace as the drum. Most lifting and winching activities should not cause any slippage. It is possible that the utilization of the capstan could be classified as static because static friction is produced when the rope rubs against the capstan in this manner. On the other hand, if the rope is allowed to slide around the drum, there will be kinetic friction,

and the system can be characterized as dynamic (Paynter, 2002).

Researchers have investigated different alterations in the Capstan amplifiers. Thomas et al. (2012) studied the characterization of a continuously variable linear force amplifier based on Capstan's theory, employing an elastic wire to enable a control actuator to declutch by releasing tension. The study shows that using a system of distributed capstan amplifiers powered by a central torque source, with cable engagement controlled by lightweight, low-torque actuators, could decrease the weight of distal actuators and enhance agility in robotic tasks. Hu et al. (2012) created a displacement amplifier to enhance the accuracy and resolution of an extensometer for measuring strain in high-temperature components. The results confirm the accuracy of the amplification ratio equation and show that the extensometer rods can exert the loading force produced by the flexure hinge's torque moment. Hu et al. (2016) developed an electrostatic sensing system to detect the lateral vibration of power transmission belts continuously and without physical touch. The results indicate that the belt vibrates at distinct modal frequencies that rise with axial speed. A shorter distance between the electrode and the belt allows for detecting higher-order vibration modes. However, it also causes significant signal distortion, resulting in higher-order harmonics.

Shahosseini and Najafi (2014) detailed the design, optimization, and testing outcomes of a mechanical amplifier connected to an electromagnetic energy harvester to produce electricity from small-amplitude (1 mm) and low-frequency (5 Hz) vibrations despite significant static displacements. The study shows that a complete electromagnetic energy harvester with this mechanical amplifier produces a high-power density of 170 W/cm3 and a 16-fold increase in output power (30 mW compared to 1.9 mW without the amplifier at 5 Hz). The capstan amplifier typically involves a rope coiled around a drum to enhance the amplification of a weight connected to one end of the rope by interacting with the tension. The likelihood of the rope getting tangled increases as more turns are added. Increased tension in the cord while binding enables the rope to securely fasten to the drum, causing the kinetic friction coefficient to surpass the static friction coefficient.

A mechanical power amplifier has a comparatively fast response time. Its continuously rotating drums allow instantaneous access to electricity. Pneumatic, hydraulic, and electrical systems need transducers to convert signals from one energy type to another when they are used for position control applications. This remains true even in the event of continuously running power sources. However, the mechanical power amplifier makes direct perception of the controlled motion possible. This study looks at assessing a power amplifier prototype's performance using the amplification factor and design optimization for several turns of rope material. The study's main goal was to calculate the amplification factor of the Capstan model mechanical power amplifier for different rope materials.

Experimental Set-Up and Construction

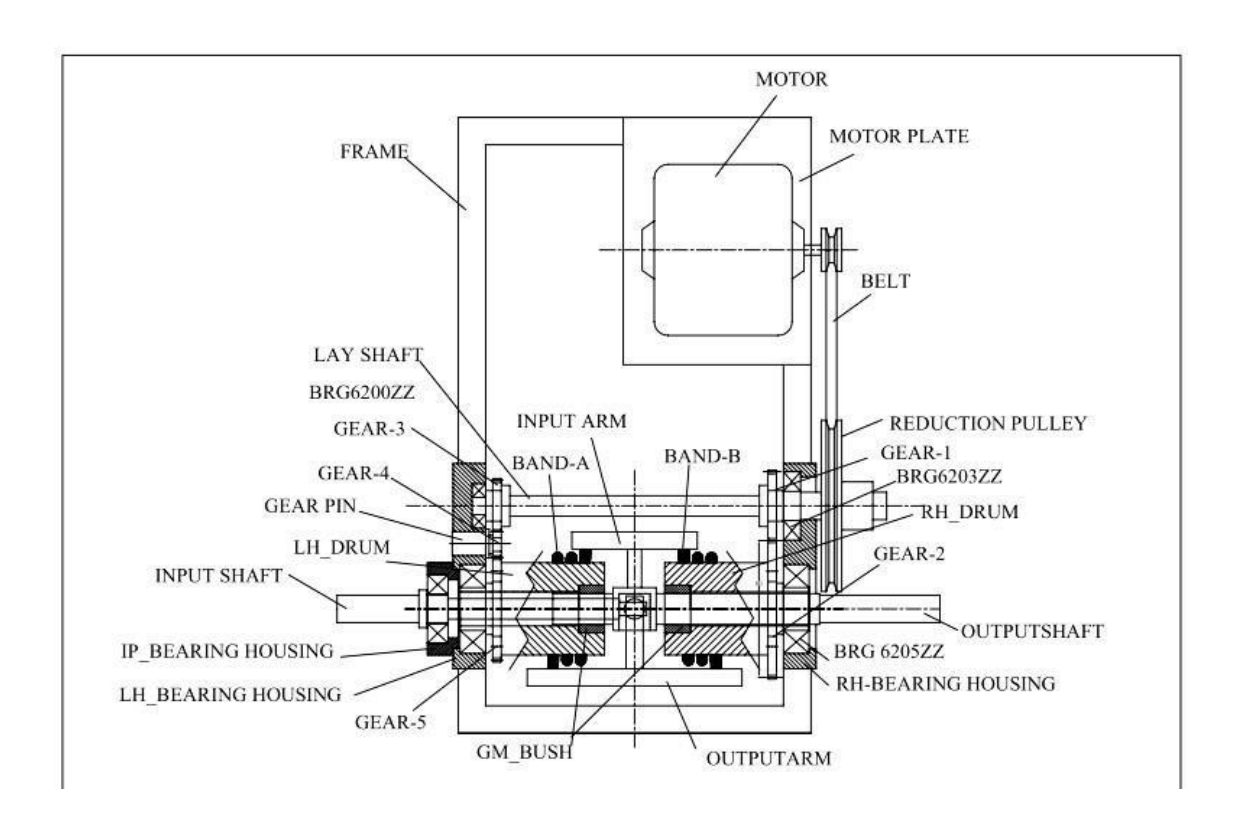


Fig. (1). Experimental set-up for capstan power amplifier.

The production overshot is halted by the drum-tightening band B around it. The slip persists until the loose end tightens. The coefficient of friction (COF) and the number of rotations impact the force required at the free end to raise the load. The power amplifier accurately adjusts the orientation of connecting bands A and B to produce an output in both directions. When the input shaft is spun clockwise (CW), the input arm takes up the slack in band A and secures it to its drum. Band A's locked end is attached to the output arm, transmitting the clockwise motion of the driven drum to the output shaft. When a flexible line is wrapped around a cylinder, the belt friction or capstan equation determines the holding and load forces relationship, such as with a bollard or winch.

A Capstan system relies on the holding force applied on one side to support a significantly larger loading force on the opposite side. Bands A and B are linked to an input shaft and arm through the power amplifier, which provides output directions and accurate angular positioning. When the input shaft is turned clockwise, the input arm tightens band A and secures it to its drum. Band A, when locked, transfers the clockwise rotation of the tail drum to the output shaft by connecting the load end of the band to the output arm. Consequently, band B becomes lethargic and stumbles over its drum. Band A slips on its drum when the input shaft stops rotating clockwise because the tension is no longer restricted. The output arm will tighten band B on the counterclockwise revolving drum and stop the shaft if it tries to rotate too quickly. The motor rotates Drum-B counterclockwise, causing the input shaft to move in the opposite direction. The diameter of the drums, the number of wraps on the bands on each drum, and the coefficient of

friction between the drum and band collectively influence the increased torque. Through the amplifier

design indicated, input power applied to the input shaft is increased and transferred to the output shaft.



Fig. (2). The prototype of Capstan mechanical power amplifier

Table 1: Capstan Mechanical Amplifier Component

1	Electrical Motor	The electrical motor has a variable speed range of 0 to 9500 rpm and has a 50-watt capacity. An electronic speed variator is used to control the speed. The motor's motor pulley provides the system's drive, and the reduction pulley is positioned on the layshaft.
2	Motor Selection	The power is transmitted to the input shaft of the amplifier using an open belt drive using two pulleys and a belt on a single-phase AC Motor with a 2 kg-cm Torque and 6000 rpm speed with 50-watt input power. The motor pulley diameter (25 mm), input shaft pulley diameter (100 mm), input speed (2100 rpm). Output speed at lay shaft (2100/4 =525), rpm Power ( $2 \times \pi \times 2100 \times .20/60 = 43.98$ W).
3	Lay Shaft	Two ball bearings installed in a bearing housing support the layshaft, built of the material EN4, and have mechanical qualities. The layshaft carries the reduction pulley and a set of gears from the gear train at one end.
4	Gear Train Specification	Gear-1: 1. 5 modules, 18 teeth, and a 5mm face width Gear-2: 1. 20 teeth, 5 modules, and a 5mm face width Gear-3: 1. 5 modules, 40 teeth, and a 5mm face width Gear-4: 1. 5 modules, 32 teeth, and a 5mm face width. Gear-5: 1. 5 modules, 64 teeth, and a 5mm face width
5	LH and RH Drums	The output shaft is supported by a gunmetal bushing attached to the left and right-hand drums, located in bearings 6005ZZ and 6005ZZ, respectively, in the bearing housing. The band is coiled around the drums and connected to the input and output arms at its two ends, respectively.
6	Input and Output Arms	The input and output arms are connected to the input shaft and output shaft. The band wound on the drums is connected to these arms at their two ends.
7	Input Shaft	The input shaft has a ball bearing 6203zz installed on one end that is retained in the input shaft housing, and the input arm is attached to the other end.
8	Output Shaft	The output shaft is placed inside the load drums by gunmetal bush bearings. One end of the output shaft is hollow so the input shaft can pass through it.
9	Frame	The frame is the part of the power amplifier that holds it all together. The LH and RH bearing housings and the motor plate are welded to the frame.
10	Rope	The rope is made of cotton beads and has a diameter of 6 mm. The left band is wound around the left drum, and the right band is wound around the right drum. Both the input and output arms are attached to the ends of these bands.

#### Test Trials and Measurement

To conduct the trial, a dyno-brake pulley cord and weight pan are provided on the output shaft. Input Data

- 1, Drive Motor < AC230 Volt 0.5 Amp, 50 watt 50 Hz, 200 to 9500 rpm (TEFC Commutator Motor)
- 2. Select the leather material for the rope and wound *three* numbers of the turn-around corresponding drums. Then, trials are conducted by the following procedure.

#### Procedure

The motor started by shifting the electronic speed variator knob to allow the mechanism to run & stabilize at a certain speed (e.g., 1300 rpm). The weight in the weight pan was attached to the input arm bracket of the LH side input shaft, and 100 gm weight was placed into the weight pan. The speed for this load was recorded using a tachometer. Also, an additional 100 gm weight was added to the weight pan. The electronic loading cell attached to the output arm bracket was mounted on the load pulley fixed on the RH side output shaft for proper recording. The input and output torque were calculated using arm length = 100 mm. Thus, the observed recording was tabulated, and Torque *versus* speed characteristics and power *versus* speed characteristics were plotted. At the same time, the steps were repeated using varying rope materials such as woolen, cotton, and steel. Finally, the sample was calculated.

Table 2 shows sample calculations for observation

Input Torque	Weight in the pan (N) Input arm length (m) = $0.1 9.81 0.10 0.0981 \text{ N-m}$
Output Torque	Electronic load cell analysis (N)×Length of output arm (m) = $0.170\times9.81\times$
	0.1 = 0.1667  N-m
Power consumed across	$2 \times \pi \times N \times T/60 = 2 \times 3.143 \times 2100 \times 0.1667 / 60 = 36.656 \text{ Watt}$
the output shaft	
Efficiency	Input / output = 36.656/ 71.56 = 51.23%

The Mechanical Power Amplifier Working Principle

The capstan model, mainly composed of two counter-rotating drums and rope coiled around it, as shown in Fig. 3, serves as the foundation for a mechanical power amplifier's operation.

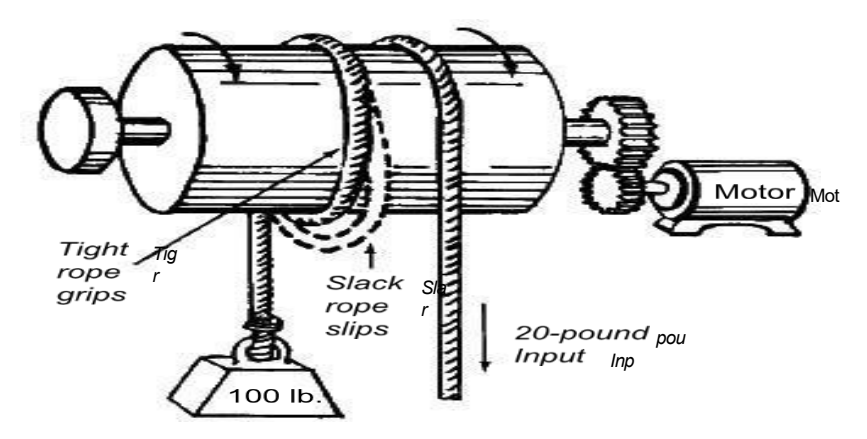


Fig. (3). Basic layout of mechanical power amplifier

Thoad □ Tholde □

where Tlaod is the actual tension on the rope line, Thold is the force that is subsequently applied on the opposite side of the capstan, is the coefficient of friction between the materials of the rope and capstan, and is the total angle swept by all turns of the rope, measured in radians (i.e., with one full turn the angle), as shown in Fig (4). From Fig. 3, it is seen that the gain in force propagates exponentially with the coefficient of friction, the number of turns, and the contact angle. Note that the cylinder radius does not influence the gain in force. Table 3 shows the factor  $e^{\mu\varphi}$  based on the number of turns and coefficient of friction.

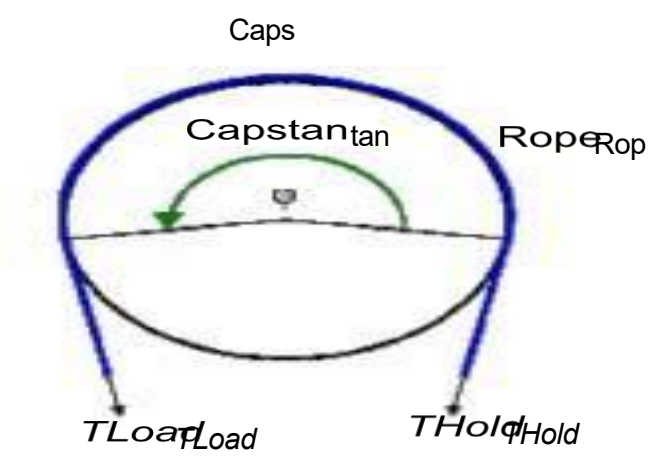


Fig. (4). Working principle of mechanical power amplifier.

Table 3. Capstan Principle.

No of rotation				Coeffi			
	0.1	0.2	0.3	0.4	0.5	0.6	0.7
1	1.9	3.5	6.6	12	23	43	81
2	3.5	12	43	152	535	1881	6661
3	6.6	43	286	1881	12392	81612	437503

Table 3 explains why a sheet, a rope attached to a sail's loose side, rarely wound more than three times around a winch. The force gain would be excessive in addition to being counterproductive because there is a chance of a riding turn, which would cause the sheet to be foul, form a knot, and not run out when relaxed (by letting go of the hold end of the tail, in land-speak). To prevent the rope (anchor warp or sail sheet) from sliding down, it is traditional in ancient and modern worlds for anchor capstans and jib winches to have a somewhat flared-out base instead of being cylindrical. If the rope is tailed (the loose end is pulled clear) by hand or with a self-trailer, it can slowly climb upwards around the winch without much chance of a riding turn. Applying this theory can create a mechanical power amplifier that amplifies the modest control force generated by an input motor. The device's output can then be utilized to demonstrate the implementation of load positioning.

## Result and Discussion

The weight pan's input weights were changed over several tests, ranging from 100 g to 1 kg; the electronic load cell's readings variations in the speed, input/output torque, power, and efficiency are documented. Table 6 summarizes the results from utilizing two numbers of turns and rope material as leather. The observations for steel and woven cotton are presented similarly in Tables 5 and 7. The relationship between speed, torque, power, and efficiency of the power amplifier assembly is displayed below. The findings are strikingly compatible with experimental measurements, including a successful computation of the amplification factor.

Table 4. Loading and unloading data

	<u> </u>	T 1'		TT11'	М С	1()	
		Loading		Unloading		peed(rpm)	
	Weight (gm)	Speed rpm		Weight (gm) Sp	eed (rpm)		
1.	100	2100	100		2100	2100	
2.	150	1960	150		1960	1960	
3.	200	1750	200		1750	1750	
4.	250	1600	250		1600	1600	
5.	300	1250	300		1250	1250	
6.	350	1050	350		1050	1050	
7.	500	810	500		810	810	
8.	600	650	600		650	650	
9.	700	535	700		535	535	
10.	800	520	800		520	520	

Table 5. Observation for power amplification factor with steel rope.

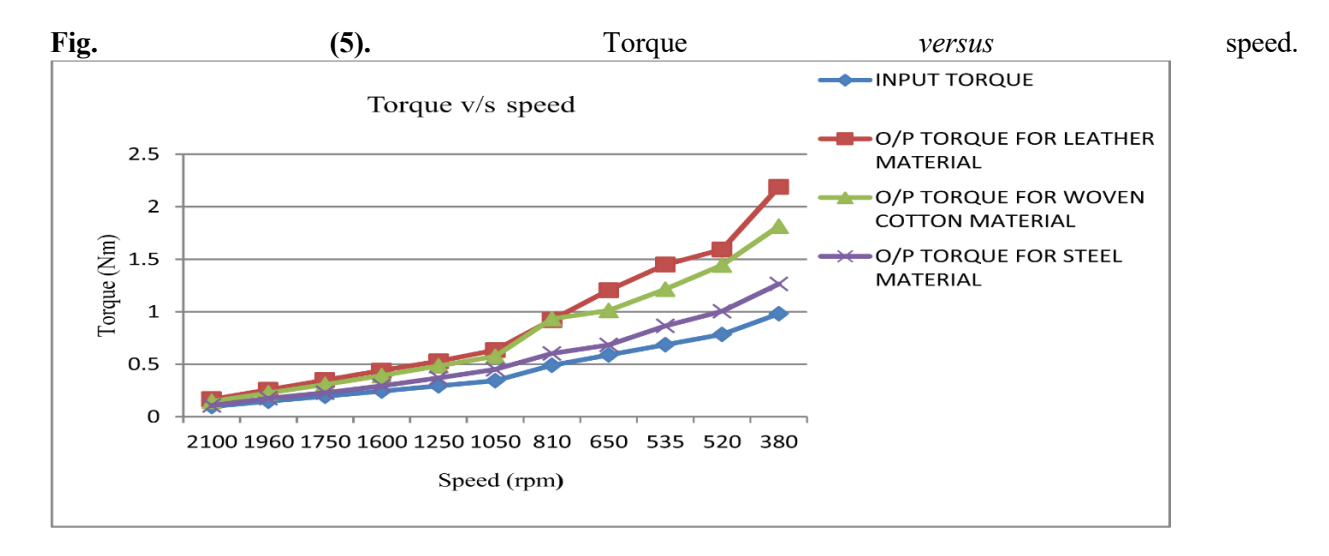
S/n	Input loa	d Load cell	Speed	Input	output arm	power co	nsumption	Power		
amp	amplification factor Efficiency									
shaft (gm) reading at output shaft		ding at	(rpm	torque (N-m)	amplified torque	(watt)	output/input torque	(%)		
1	100	110	2100	0.0981	0.10791	23.718618	1.1	33.1439		
2	150	180	1960	0.14715	0.17658	36.2247984	1.2	45.17521		
3	200	233.3334	1750	0.1962	0.22890006	41.92686198	1.166667	48.7877		
					5					
4	250	300	1600	0.24525	0.2943	49.28544	1.2	54.11748		
5	300	378	1250	0.2943	0.370818	48.515355	1.26	54.81697		
6	350	460.8334 5	1050	0.34335	0.45207761 4	49.68332983	1.316667	56.629		
7	500	614.2855	810	0.4905	0.60261407 6	51.08962132	1.228571	55.7840		
8	600	697.5	650	0.5886	0.6842475	46.55163825	1.1625	51.6985		
9	700	882	535	0.6867	0.865242	48.45066786	1.26	54.7756		
10	800	1024	520	0.7848	1.004544	54.67398144	1.28	58.9705		
11	1000	1290	380	0.981	1.26549	50.3327556	1.29	56.54245		

Table 6. Observation for power amplification factor with leather rope.

S/n	Input load shaft (gm)	Load cell reading at output shaft	Speed (rpm)	Input torque (N-m)	output arm amplified torque	power consumption (watt)	Power amplification factor output/input torque	or Efficiency (%)
1	100	170	2100	0.0981	0.16677	36.656046	1.7	51.22250825
2	150	262.5	1960	0.14715	0.2575125	52.827831	1.75	65.88051963
3	200	356	1750	0.1962	0.349236	63.968394	1.78	74.43612261
4	250	450	1600	0.24525	0.44145	73.92816	1.8	81.17622256
5	300	540	12500	2943	0.52974	69.30765	1.8	78.30996817
6	350	647.5	1050	0.34335	0.6351975	69.80820525	1.85	79.56786874
7	500	940	810	0.4905	0.92214	78.1790292	1.88	85.36264583
8	600	1230	650	0.5886	1.20663	82.091061	2.05	91.16729388
9	700	1477	535	0.6867	1.448937	81.13564221	2.11	91.72749805
10	800	1624	520	0.7848	1.593144	86.70951744	2.03	93.52360221
11	1000	2230	380	0.981	2.18763	87.0093372	2.23	97.74392716

Table 7. Observation for power amplification factor with woven cotton rope.

S/n	Input load	Load cell	Speed	Input	output arm	power consumption	Power amplification		Efficiency
	shaft (gm)	reading at output shaft	(rpm)	torque (N-m)	amplified torque	(watt)	output/input torq	ue	(%)
1	100	150	2100	0.0981	0.14715	32.34357	1.1	45.196	533081
2	150	232.5	1960	0.14715	0.2280825	46.7903646	1.3	58.351	131739
3	200	314	1750	0.1962	0.308034	56.421561	1.433333	65.654	133287
4	250	400	1600	0.24525	0.3924	65.71392	1.5	72.156	664228
5	300	495	1250	0.2943	0.485595	63.5320125	1.6	71.784	113748
6	350	588	1050	0.34335	0.576828	63.3933972	1.75	72.256	522675
7	500	850	810	0.4905	0.83385	70.693803	1.857143	77.189	962655
8	600	1032	650	0.5886	1.012392	68.8764024	1.5625	76.491	158315
9	700	1239	535	0.6867	1.215459	68.06165247	1.48	76.946	676376
10	800	1472	520	0.7848	1.444032	78.59384832	1.39	84.770	)1616
11	1000	1850	380	0.981	1.8 <b>74</b> 85	72.182634	1.2	81.088	301132



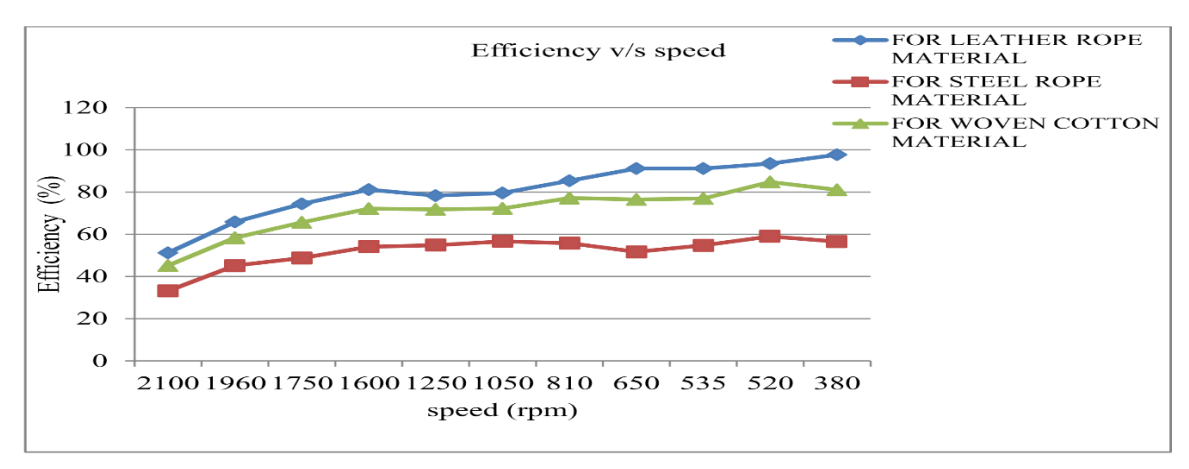


Fig. (6). Efficiency versus speed.

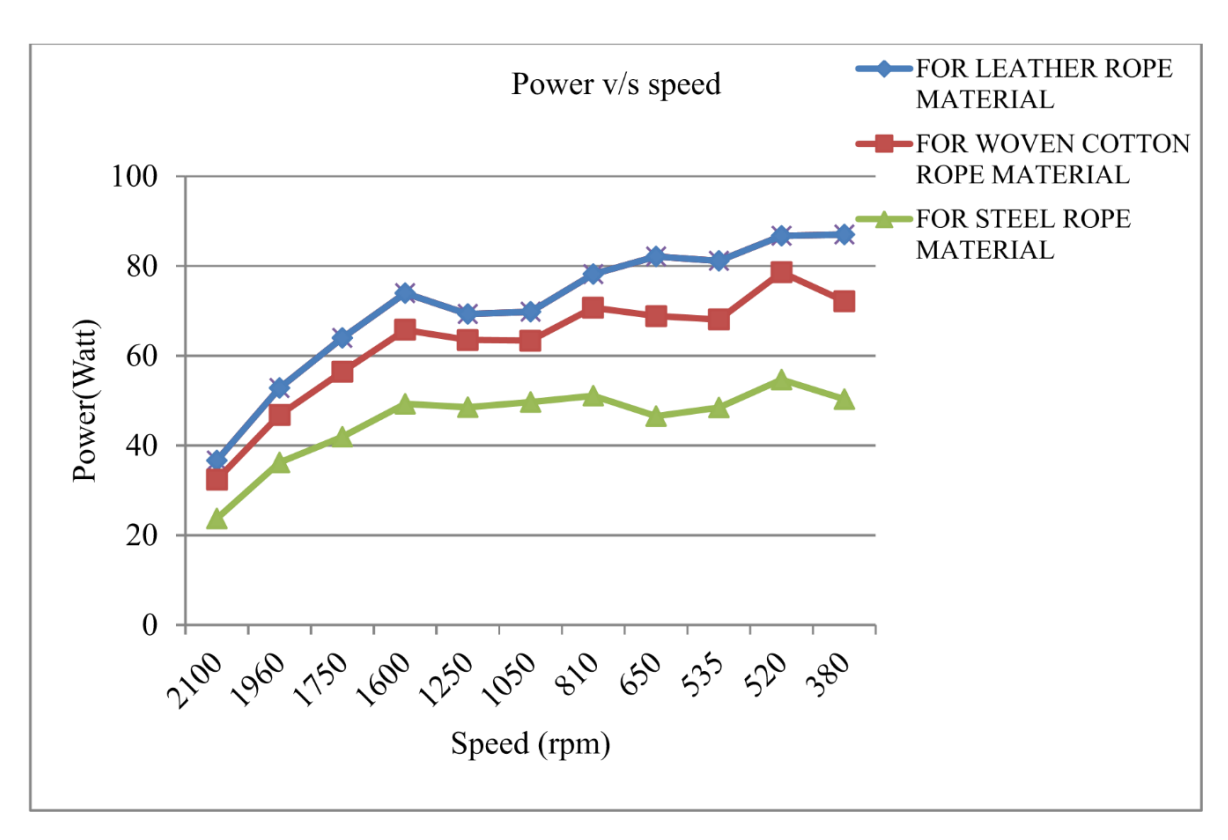


Fig. (7). Power versus speed.

It can be noted from Fig. (5) that when the speed decreases, the torque recorded at the input shaft increases due to the increased input load. It is also noted that as the speed decreases, the measured torque at the output shaft increases. The relationship between torque and speed is inverse, although the amplification factor increases as speed drops. The maximum value of the amplification factor is 2.23 for leather rope, 1.867 for woven cotton, and 1.32 for steel at low speeds with correspondingly large torque values. Very little variety remains in the values of the amplification factor. Maximum output torque is attained at 380 revolutions per minute, equaling

2.18 Newton meters for leather, 1.266 Newton meters for steel rope, and 1.815 Newton meters for woven rope.

As shown in Fig. 6, system efficiency rises as speed falls. As a result, efficiency is poor, yet initial speed is high. The efficiency of several power transmission systems, such as the belt drive and gear system, declines as the system's load grows; as a result, the system's total efficiency drops after a certain threshold. At 230 rpm and 1000 g input weight, leather rope material achieves a maximum efficiency of 97.74 percent. Similar to this, woven cotton has a maximum efficiency of 84.87 percent at 520 revolutions per minute and 800 grams. Steel rope material has 520 spins per minute and weighs 800 grams.

As speed decreases, it can be seen from Fig. 7 that power over the system's output shaft increases. As a result, at first, power is low, and speed is high. Power across the output shaft increases when load increases, speed across the shaft decreases, and vice versa. The maximum power at the output arm for leather rope is 87.008 watts, compared to 78.59 watts for woven cotton rope and 54.67 watts for steel. According to experimental studies, a mechanical power amplifier's performance can be improved by raising its amplification factor. The following variable affects the amplifying factor. It is based on the

number of rope rotations and the angle at which the rope is wrapped around the capstan drum. The number of turns has an exponential relationship with the amplification factor. However, going beyond two or three spins will result in the rope tangled around the revolving drum, reducing the amount of kinetic energy the drum receives from the electric motor drive. It leads to decreased transmission power and efficiency, producing ludicrous outcomes. Given this, choosing the ideal number of turns, two or three will produce the appropriate outcomes. It also depends on the friction between the rope and the drum. Power amplification can be improved by choosing an elastic rope material with a high coefficient of friction. It is clear that among the other materials, such as woven cotton and steel, the leather- to-steel rope-drum pair has the highest coefficient of friction (0.6).

#### Conclusion

The primary purpose of this work was to calculate the amplification factor of mechanical power amplifiers for various rope materials such as leather, woven cotton, and steel rope. An intensive combination of analytical and experimental research was utilized to accomplish this goal. The experimental study verifies that maintaining an optimal number of turns equal to two results in a power amplification factor of 2.23 for leather contact, 1.867 for woven cotton contact, and 1.32 for steel contact of rope. This is the case when the optimal number of turns is maintained. It is clear from these results that the power amplification of leather is superior to that of woven cotton and steel. The results showed a remarkable consistency with the experimental measurements, including a positive estimate for the amplification factor.

#### References

- Baser, O., & Ilhan Konukseven, E. (2010). Theoretical and experimental determination of capstan drive slip error. *Mechanism and Machine Theory*, 45(6). https://doi.org/10.1016/j.mechmachtheory.2009.10.013
- Bienert, F., Loescher, A., Röcker, C., Graf, T., & Ahmed, M. A. (2022). Experimental analysis on CPA-free thin-disk multipass amplifiers operated in a helium-rich atmosphere. *Optics Express*, *30*(21). https://doi.org/10.1364/oe.469697
- Choi, H. (2023). A Doherty Power Amplifier for Ultrasound Instrumentation. *Sensors*, *23*(5). https://doi.org/10.3390/s23052406
- Gawande, S. H. (2018). Performance Evaluation of Mechanical Power Amplifier for Various Belt Materials. *The Open Mechanical Engineering Journal*, 12(1). https://doi.org/10.2174/1874155x01812010095
- Hu, X. Y., Jia, J. H., & Tu, S. T. (2012). Displacement amplifier design for an extensometer in high-temperature deformation monitoring. *Procedia Engineering*, 29.https://doi.org/10.1016/j.proeng.2012.01.229
  - Hu, Y., Yan, Y., Wang, L., & Qian, X. (2016). Non-Contact Vibration Monitoring of Power Transmission Belts Through Electrostatic Sensing. *IEEE Sensors Journal*, 16(10). https://doi.org/10.1109/JSEN.2016.2530159
  - Jeong, H., Lee, H. D., Park, B., Jang, S., Kong, S., & Park, C. (2023). Three-Stacked CMOS Power Amplifier to Increase Output Power With Stability Enhancement for mm-Wave

- Beamforming Systems. *IEEE Transactions on Microwave Theory and Techniques*, 71(6). https://doi.org/10.1109/TMTT.2022.3228539
- Li, K., Li, J. H., Li, L., Zhuo, Y., Pan, B., & Fu, Y. L. (2022). Mechanism synthesis and kinematic analysis of 4-DOF minimally invasive surgical instrument. *Zhejiang Daxue Xuebao (Gongxue Ban)/Journal of Zhejiang University (Engineering Science)*, 56(6). https://doi.org/10.3785/j.issn.1008-973X.2022.06.008
- Paynter, H. M. (2002). The differential analyzer is an active mathematical instrument. *IEEE Control Systems Magazine*, 9(7). https://doi.org/10.1109/37.41449
- Qi, F., Ju, F., Bai, D., Wang, Y., & Chen, B. (2018). Motion modeling and error compensation of a cable-driven continuum robot for applications to minimally invasive surgery. *International Journal of Medical Robotics and Computer Assisted Surgery*, 14(6). https://doi.org/10.1002/rcs.1932
- Schumann, P., Zöllner, R., & Schmidt, T. (2022). A new model and alternative solutions for describing double-layered flexible elements wrapped around a cylinder. *Mechanism and Machine Theory*, 172. https://doi.org/10.1016/j.mechmachtheory.2022.104823
- Shahosseini, I., & Najafi, K. (2014). Mechanical amplifier for translational kinetic energy harvesters. *Journal of Physics: Conference Series*, 557(1). https://doi.org/10.1088/1742-6596/557/1/012135
- Starkey, M. M., & Williams, R. L. (2011). Capstan as a mechanical amplifier. *Proceedings of the ASME Design Engineering Technical Conference*, 6(PARTS A AND B). https://doi.org/10.1115/DETC2011-48262
- Thokale M. J. (2016). Mechanical power amplifier working on a capstan principle. Ijariie. Vol-2 Issue-4
- Thomas, G. C., Gimenez, C. C., Chin, E. D., Carmedelle, A. P., & Hoover, A. M. (2012). Controllable, high force amplification using elastic cable capstans. *Proceedings of the ASME Design Engineering Technical Conference*, 4(PARTS A AND B). https://doi.org/10.1115/DETC2012-71295
- Wang, Z., Hu, S., Gu, L., & Lin, L. (2022). Review of Ka-Band Power Amplifier. In *Electronics (Switzerland)* (Vol. 11, Issue 6). https://doi.org/10.3390/electronics11060942

# Construction of Water Level Indicator with Microprocessor using Seven Segment Display

Engr. Joshua Okoekhian

Department of Electrical/Electronic Engineering Technology, National Institute of Construction Technology and Management, Uromi, Edo State, Nigeria.

j.okoekhian@nict.edu.ng

#### **Abstract**

This project focuses on the construction of a water level indicator using an ATtiny84 microcontroller and a seven-segment display to provide a reliable and efficient solution for monitoring water levels. The primary objective was to create a user-friendly system that accurately detects water levels ranging from empty (0) to full (9) and displays this information in real-time. The system comprises a 12V power adapter, an LM7805 voltage regulator to provide a stable 5V power supply, conductive water level sensors, and a seven-segment display. The ATtiny84 microcontroller was programmed using the Arduino IDE to read inputs from the water level sensors, process these inputs, and control the display. The design ensures precise water level detection and display, with the microcontroller efficiently managing the sensor data and updating the seven-segment display accordingly. Current-limiting resistors were employed to protect the LEDs in the display, enhancing the system's durability. Extensive testing and calibration confirmed the system's accuracy and reliability, demonstrating its potential for various applications such as water tanks, reservoirs, and aquariums. This project not only provides a practical solution for water level monitoring but also serves as an educational tool, illustrating the integration of microcontrollers, sensors, and displays in embedded systems. The successful implementation of this project highlights the effectiveness of microcontroller-based designs in achieving real-time monitoring and control, and it sets the stage for future enhancements such as wireless connectivity and remote monitoring capabilities.

**Keywords**: Water Level Indicator, ATtiny84 Microcontroller, Seven Segment Display, Conductive Sensors

# I. Introduction

The increasing urbanization and population growth have necessitated the development of effective water management systems. Among these systems, water level indicators play a crucial role in monitoring and managing water resources in various applications such as water tanks, reservoirs, and aquariums. These systems are essential for ensuring efficient water use, preventing overflow, and detecting leaks, thereby contributing to sustainable water management practices. The integration of microcontrollers in such systems has further enhanced their efficiency, accuracy, and reliability (Gleick, 2003). Microcontrollers offer better solution, being computers on single chips; enable production of embedded smart systems which are prevalent everywhere today (Bales, 2008; Akinwole, 2020). Efficient use and water monitoring, have

necessitated research into various water level sensing technologies, and collection methods (Khaled et al., 2010; Venkata, 2013; Hodgson & Walters, 2002; Kehinde et al., 2016).

The history of water level monitoring can be traced back to ancient civilizations, where simple mechanical devices were used to measure and control water levels in irrigation systems and reservoirs. However, the advent of electronics and microcontrollers has revolutionized this field, providing more accurate and automated solutions. The development of microcontroller-based water level indicators has been driven by the need for more efficient, reliable, and cost-effective solutions. These systems use various types of sensors to detect water levels and provide real-time data, which can be used for monitoring and control purposes (Gleick, 2003).

Microcontrollers, such as the ATtiny84 have become popular in water level indicator systems due to their versatility, low power consumption, and ease of programming. The ATtiny84 is a powerful yet compact microcontroller that offers a range of features, including multiple I/O pins, analog-to-digital conversion, and programmable memory, making it suitable for various applications. Its small size and low cost make it an ideal choice for embedded systems, where space and budget constraints are significant considerations (Atmel, 2006).

The choice of sensors is critical in the design of a water level indicator. Conductive water level sensors are commonly used due to their simplicity and reliability. These sensors consist of multiple conductive tracks or probes that detect the presence of water through its conductivity. When water contacts the probes, it completes an electrical circuit, generating a digital signal that can be read by the microcontroller. This type of sensor is particularly suitable for applications where the water quality is consistent and the risk of corrosion is low (Morris & Langari, 2012).

The testing and calibration of the water level indicator system are crucial to ensure its accuracy and reliability. The sensor probes must be placed at appropriate levels in the water container to provide accurate readings. The system is tested by varying the water level and observing the output on the seven-segment display. Any discrepancies or issues are addressed by adjusting the code or the hardware connections. This iterative process ensures that the system operates reliably under different conditions and provides accurate water level measurements (Maxfield, 2009).

The development of microcontroller-based water level indicators is part of a broader trend towards the automation and digitalization of water management systems. These systems offer numerous advantages, including improved accuracy, real-time monitoring, and the ability to integrate with other digital systems for data analysis and control. The use of microcontrollers allows for greater flexibility and customization, enabling the development of tailored solutions for specific applications. As the demand for efficient water management continues to grow, the adoption of microcontroller-based systems is expected to increase (Gleick, 2003).

The implementation of a water level indicator system has significant implications for water conservation and management. By providing accurate and real-time data on water levels, these systems enable better decision-making and more efficient use of water resources. For example, in agricultural settings, water level indicators can help optimize irrigation schedules, reducing water waste and improving crop yields. In residential and commercial buildings, these systems can prevent water damage by detecting leaks and overflow, contributing to cost savings and environmental sustainability (Morris & Langari, 2012).

The use of seven-segment displays in water level indicators provides a simple and effective way to visually represent water levels. These displays are widely used in digital clocks, calculators, and other electronic devices due to their simplicity and readability. By combining the ATtiny84 microcontroller with a seven-

segment display, this project aims to create a reliable and user-friendly water level indicator that can be easily integrated into various water management systems.

#### II. MATERIALS AND METHODS

#### **Materials**

The following materials were used for the construction of the project:

# i. Seven Segment Display

The seven-segment display is an essential component in the water level indicator project, designed for displaying decimal numerals using seven individual LED segments arranged to form the shape of the number "8." Each segment can be illuminated in various combinations to represent numbers from 0 to 9, with an additional segment for the decimal point. The display types include common anode (CA) and common cathode (CC), differing in how the LEDs are connected to power and ground. In this project, the seven-segment display was connected to an ATtiny84 microcontroller, which controls the segments by sending signals to display the appropriate digit for the detected water level. This setup provides a clear visual representation of the water level, making it ideal for educational and prototype applications. The display's simplicity, cost-effectiveness, and compatibility with microcontrollers make it a popular choice for projects requiring numerical displays. Figure 1 is a presentation of a seven segment display.

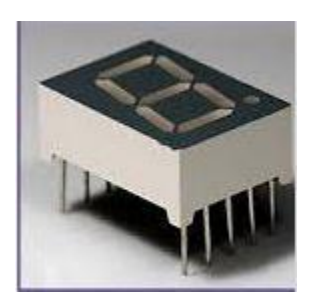


Figure 1: Seven segment display

# ii. ATtiny84 Microcontroller

The ATtiny84 microcontroller is a crucial component in this project, providing the necessary computational power and versatility to manage the system's operations. This 14-pin, 8-bit microcontroller from Microchip Technology offers a compact and efficient solution for small-scale projects, featuring 12 digital I/O pins and 8 analog inputs. It operates within a voltage range of 1.8V to 5.5V, making it compatible with a variety of power sources, including the 5V regulated supply from an LM7805 voltage regulator used in this project. The ATtiny84 includes 8 KB of Flash memory, 512 bytes of SRAM, and 512 bytes of EEPROM, providing ample space for program storage and data handling. Its clock speed can reach up to 20 MHz with an external crystal, though for this project, an internal clock might suffice, simplifying the design. The microcontroller was programmed using the Arduino IDE, which supports ATtiny microcontrollers, enabling easy development and uploading of code via an ISP programmer. In this project, the ATtiny84 reads inputs from the water level sensor module, processes these inputs to determine the current water level, and drives a seven-segment display to visually indicate this level. The digital I/O pins of the ATtiny84 are used to control the individual segments of the display through currentlimiting resistors and transistors for sufficient current drive. Its analog input pins could also be used if the water level sensors provide analog signals, although digital input is more common for such sensors. The ATtiny84's low power consumption and compact size make it ideal for embedding into the breadboardbased circuit, ensuring the project remains streamlined and efficient. The ATtiny84 microcontroller's

combination of sufficient I/O capabilities, ease of programming, and compatibility with common sensors and displays makes it an excellent choice for implementing a robust and reliable water level indicator system. Figure 2 is a presentation of an ATtiny84 microcontroller.

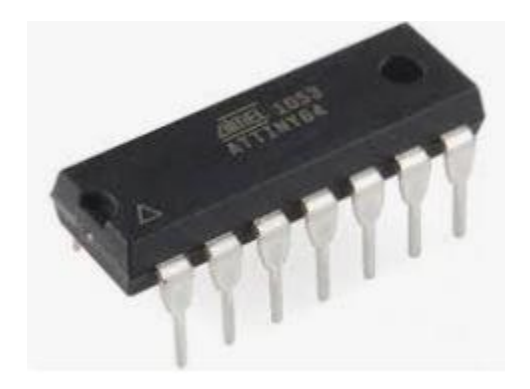


Figure 2: ATtiny84 Microcontroller

#### iii. Water Level Sensor Module

The water level sensor module is a pivotal component in the construction of this project, offering a reliable means of detecting water levels and providing corresponding digital signals to the ATtiny84 microcontroller. This sensor typically consists of multiple exposed conductive tracks or probes arranged at different heights, which detect the presence of water through conductivity. When water contacts these tracks, it completes an electrical circuit, generating a HIGH or LOW digital signal based on the water level. The module operates within a voltage range of 3.3V to 5V, making it directly compatible with the ATtiny84 microcontroller's power requirements, provided by a 5V regulated supply from an LM7805 voltage regulator. This compatibility ensures seamless integration into the breadboard-based circuit. The sensor's outputs are connected to the digital input pins of the ATtiny84, which reads the signals to determine the current water level. The microcontroller processes these inputs to control the seven-segment display, visually indicating the water level. By detecting the presence of water at different levels, the sensor module ensures accurate and real-time water level monitoring. Its ease of use and integration with microcontrollers like the ATtiny84 highlight its versatility in electronics projects.

# iv. Power Supply

The 12V power adapter and the LM7805 voltage regulator were used in the power supply unit in order to ensure a stable and reliable power supply for the circuit. The 12V power adapter converts standard AC voltage from a power outlet into 12V DC, which is a suitable input for the voltage regulator. The LM7805 voltage regulator then steps down this 12V DC to a stable 5V DC, which is necessary for powering the ATtiny84 microcontroller and other components such as the seven-segment display and water level sensor module. This regulated 5V output ensures that the sensitive electronic components receive a consistent voltage, preventing potential damage from fluctuations and providing reliable operation. The LM7805 is a linear regulator known for its simplicity and efficiency in providing a fixed output voltage. It typically requires input and output capacitors to stabilize the voltage and filter out noise, ensuring smooth and stable operation. By using the 12V power adapter in conjunction with the LM7805, the project achieved a robust power solution that supports the microcontroller's voltage requirements, enhancing the overall reliability and performance of the water level indicator system.

#### v. Others

The following were other materials used for the construction of the project:

- a. Breadboard
- b. Connecting Wires
- c. Resistors
- d. Transistors
- e. Capacitors

#### Methods

The process began with defining the project requirements and selecting the appropriate components. The core of the system is the ATtiny84 microcontroller, chosen for its compact size, sufficient I/O pins, and ease of programming using the Arduino IDE. First, the power supply subsystem was designed. A 12V power adapter was selected to convert the AC mains voltage to 12V DC. This 12V output was then fed into an LM7805 voltage regulator, which steps down the voltage to a stable 5V DC. This regulated 5V is essential for powering the ATtiny84 microcontroller and other electronic components, ensuring consistent operation without damaging sensitive parts. Input and output capacitors were connected to the LM7805 to filter out noise and stabilize the voltage. Figure 3 presents a block diagram of the system.

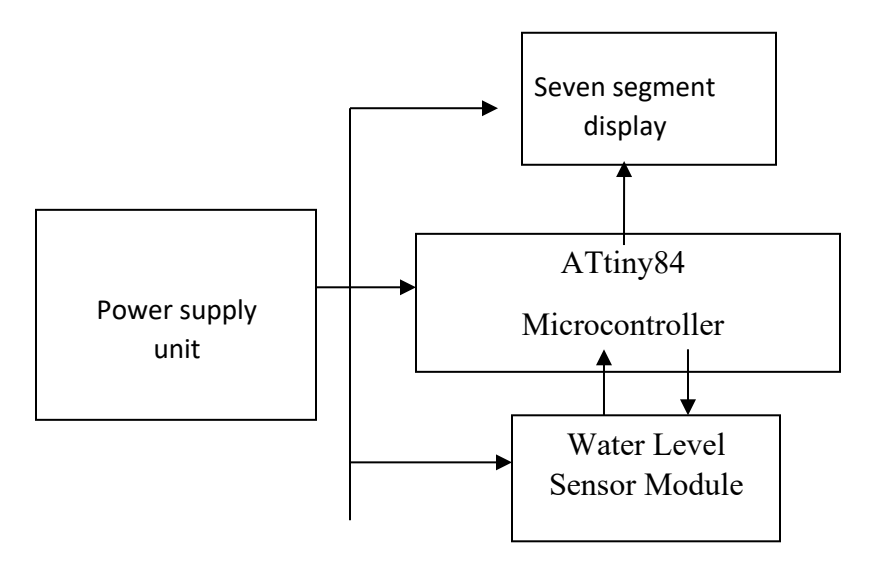


Figure 3: Block Diagram of the Water Level Indicator System

Next, the water level sensor module was integrated into the design. This sensor, which typically consists of multiple conductive tracks or probes, detects the water level based on the conductivity of the water. The sensor provides digital signals indicating different water levels, which are fed into the digital input pins of the ATtiny84 microcontroller. The water level is measured on a scale from 0, indicating an empty state, to 9, signifying full capacity. Proper placement of the sensor in the water container ensures accurate detection of varying water levels.

The design then focuses on the seven-segment display, which visually represents the detected water level. The display was connected to the digital output pins of the ATtiny84 through current-limiting resistors to protect the LEDs from excessive current. The ATtiny84 was programmed to control the display, lighting up specific segments to form numerals (0 to 9) corresponding to the water level.

The wiring and interconnections were then carefully planned and executed on a breadboard. This temporary setup allows for easy adjustments and troubleshooting. The power supply, microcontroller, water level

sensor, and seven-segment display are all interconnected with appropriate wiring, ensuring that signals and power are correctly distributed across the system.

Programming the ATtiny84 is a crucial step in the design process. Using the Arduino IDE, the microcontroller was coded to read inputs from the water level sensor and output the corresponding digit to the seven-segment display. The code includes functions to initialize the I/O pins, read sensor data, process this data to determine the water level, and control the display segments accordingly. The program was uploaded to the ATtiny84 using an ISP programmer. The code used for the system is presented below:

```
// Define the pins for the seven-segment display segments
const int segmentPins[7] = \{2, 3, 4, 5, 6, 7, 8\}; // PA0 to PA6
// Define the pins for the water level sensors
const int sensorPins[10] = {9, 10, 11, 12, 13, 0, 1, 3, 4, 5}; // PB0 to PB2 and PA7 to PA5
// Segment patterns for digits 0-9
const byte digits[10] = {
 B00111111, // 0
 B00000110, // 1
 B01011011, // 2
 B01001111, // 3
 B01100110, // 4
 B01101101, // 5
 B01111101, // 6
 B00000111, // 7
 B011111111, // 8
 B01101111 // 9
};
void setup() {
// Set the segment pins as outputs
 for (int i = 0; i < 7; i++) {
  pinMode(segmentPins[i], OUTPUT);
 // Set the sensor pins as inputs
 for (int i = 0; i < 10; i++) {
  pinMode(sensorPins[i], INPUT);
}
void loop() {
 // Read water level
 int level = readWaterLevel();
 // Display the water level
 displayDigit(level);
 delay(1000); // Update the display every second
}
int readWaterLevel() {
 // Iterate through sensor pins and return the highest level detected
```

```
for (int i = 9; i >= 0; i--) {
   if (digitalRead(sensorPins[i]) == HIGH) {
     return i + 1;
   }
}
return 0; // Return 0 if no water is detected
}

void displayDigit(int digit) {
   // Display the corresponding digit on the seven-segment display
   byte pattern = digits[digit];
   for (int i = 0; i < 7; i++) {
     digitalWrite(segmentPins[i], bitRead(pattern, i));
   }
}</pre>
```

# III. Results and Discussion

The construction and testing of the water level indicator project using an ATtiny84 microcontroller and a seven-segment display yielded positive results, demonstrating both functionality and reliability. The system effectively monitored water levels from 0 (empty) to 9 (full) and displayed the corresponding digit on the seven-segment display. Each segment of the display was properly illuminated to represent the detected water level, indicating that the integration of the microcontroller with the sensor module and display was successful. Figure 4 and 5 presents the water level indicator system at different levels.

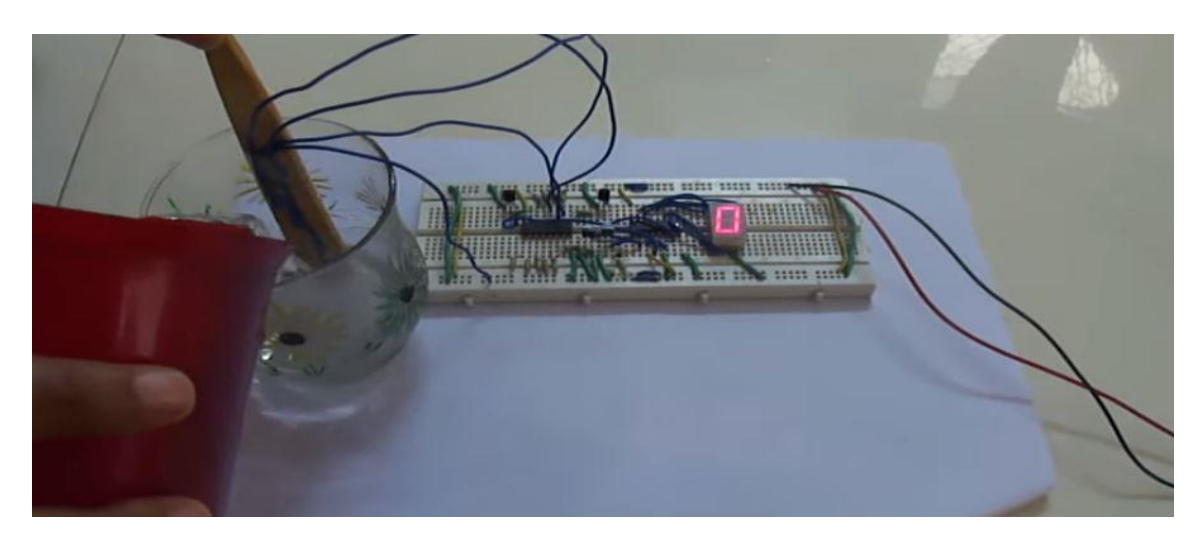


Figure 4: Water Level Indicator System at Level 0



Figure 4: Water Level Indicator System at Level 1

During testing, the water level sensors accurately detected different water levels and provided the correct digital signals to the ATtiny84. The microcontroller processed these inputs efficiently and updated the display in real-time, reflecting the current water level without noticeable delay. This real-time response is crucial for applications where immediate water level monitoring is required. The use of current-limiting resistors ensured that the LEDs in the seven-segment display operated safely, preventing any damage due to excessive current.

The power supply unit, comprising a 12V power adapter and an LM7805 voltage regulator, provided a stable 5V output necessary for the microcontroller and other components. The regulated power supply was essential for maintaining consistent operation, as fluctuations in voltage could have led to incorrect readings or potential damage to the microcontroller and LEDs. The LM7805 performed well under load, with the capacitors effectively filtering out any noise and stabilizing the output voltage.

However, a few challenges were encountered during the project. Initial calibration of the water level sensors was required to ensure accurate detection across all levels. Variations in sensor placement or slight differences in conductivity of the water could affect the readings, necessitating careful calibration. Additionally, the physical setup on the breadboard, while convenient for prototyping, introduced some instability in connections. This was mitigated by ensuring all connections were secure and stable, and by planning for a more permanent setup such as soldering components onto a PCB for future iterations.

# I. Conclusion

The water level indicator project using an ATtiny84 microcontroller and a seven-segment display successfully achieved its objective of providing an efficient and reliable method for monitoring and displaying water levels. The project demonstrated the effective integration of various components, including the power supply, sensor module, and display unit, to create a cohesive and functional system. The choice of the ATtiny84 microcontroller proved to be appropriate for this application, offering sufficient I/O capabilities and ease of programming.

The system's ability to provide accurate real-time water level readings highlights its potential utility in various practical applications, such as monitoring water tanks, aquariums, and other liquid storage

environments. The simplicity of the design, combined with the low cost and availability of components, makes this project accessible for educational purposes and small-scale implementations. Additionally, the project laid a foundation for further enhancements, such as adding wireless capabilities or integrating more advanced sensors, which could extend its functionality and usability.

# Acknowledgement

The author gratefully acknowledges the management of NICTM and TETFUND for their invaluable support and funding, which made this project possible.

## Reference

Akinwole, O. O. (2020). Design, simulation and implementation of an Arduino microcontroller based automatic water level controller with I2C LCD display. International Journal of Advances in Applied Sciences (IJAAS), 9(2), 77-84.

Atmel. (2006). ATtiny24/44/84 Datasheet. Atmel Corporation.

Bates, M.P. (2008.). Programming 8-bit PIC microcontrollers in C with interactive hardware simulation, NewnessUSA,

Gleick, P. H. (2003). Water Use. Annual Review of Environment and Resources, 28(1), 275-314.

Hodgson, J., & Walters, T. (2002). Optimizing pumping systems to minimize first or life-cycle cost. Proceedings of the  $19^{th}$  international pump users symposium, pp. 1-8

Kehinde, O. O., Bamigboye, O. O., & Ehiagwina, F. O. (2016). Design and implementation of an AT89C52 microcontroller based water pump controller. International Journal of Innovative Science, Engineering & Technology (IJISET), 3(7).

Khaled, R. S., Shah, A. M., & Mohsin, R. (2010). Microcontroller Based Automated Water Level Sensing and Controlling: Design and Implementation Issue. Proceedings of the World Congress on Engineering and Computer Science, pp. 220-224

Maxfield, C. (2009). Bebop to the Boolean Boogie: An Unconventional Guide to Electronics (3rd ed.). Newnes.

Morris, A. S., & Langari, R. (2012). Measurement and Instrumentation: Theory and Application. Academic Press.

Venkata, N. G. (2013). Microcontroller based automatic plant irrigation system. International Journal of Advancements in Research & Technology, 2(4).

Application of Solidworks Simulation to Improve Mechanical Design Skills of Mechanical EngineeringStudents in the National Institute of Construction Technology and Management, Edo State, Nigeria.

Agbonkhese Ason Kingsley<sup>1</sup>; Okojie Godwin<sup>2</sup>; Agbadua Udukhomoshi Timothy<sup>3</sup>

1,2,3 E-mail: k.agbonkhese@nict.edu.ng; g.okojie@nict.edu.ng; u.timothy@nict.edu.ng

<sup>1,2,3</sup>Department of Mechanical Engineering Technology National Institute of Construction Technology and Management, Uromi, Edo State, Nigeria

# **Abstract**

Solid Works, a comprehensive 3D CAD design solution, equips the product design team withall the necessary tools for mechanical designs, verifications, motion simulations, data management, and communication. This paper delves into Solidworks as pedagogical simulation software, a practical tool that can significantly enhance the mechanical design skills of mechanical engineering students at the National Institute of Construction Technology and Management, Edo State, Nigeria. The study was structured as an educational design experiment, utilizing Solidworks to teach design concepts. Two equivalent groups were formed; one was the experimental group, and the other was the control group. Both groups were given the same project, with the first group using SW-P and the second group using the traditional method. The results showed that Solidworks is an efficient method for enhancing mechanical design skills. Students using Solidworks demonstrated a deeper understanding of the design concepts, surpassing those using the traditional method.

Keywords: Solidworks, mechanical design, skills, mechanical engineering

# Introduction

Mechanical engineering design is the heart of innovation that emphasizes creating, improving, and optimizing machines, components, and systems. Notably, mechanical engineering design entails identifying and solving engineering problems. Although engineering design can take many forms, it is all based on processes. The mechanical design consists of conceptualizing, modeling, and improving mechanical systems. Mechanical

engineers are essential in realizing complex concepts, including the design of state-of-theart automobiles, space probes, and even basic gear mechanisms. Mechanical engineering design is a dynamic field that requires a blend of technical expertise, creativity, and problemsolvingabilities. Engineering design courses provide a platform for educators to prepare students with skills and experience in design concepts (Perez et al., 2021).

Insinuations suggest that a growing number of graduates from the mechanical engineering field were not developing the necessary skills needed in the engineering ecosystem. For instance, (Kuppuswamy & Mhakure, 2020; and Yavuzcan and Gür 2020) noted that most engineering education institutions produce great scientists knowledgeable in engineering science, mathematics, analytical techniques, and research but lack the needed skills in engineering designs. Similarly, Cohen and Katz (2015) stated that the mechanical engineering curriculum of many institutions does not include courses that teach students essential professional knowledge needed to become a design engineer. Students who graduatefrom engineering programs should be prepared to meet the demands of the industry because most engineering jobs involve both designing and practicing.

The use of a wide range of diverse meanings, spaces, processes, and instructional techniques to gain a global perspective on creating the student learning experience is becoming more andmore common in research on digital learning (Philippe et al., 2020). Because of recent advancements in computer technology, the fields of science and engineering have become very dynamic. These advancements have produced numerous computer programs to tackle classic and new problems. These applications help design, develop, and control complex systems using the computer's enhanced computational capabilities. Most subjects taught in science education have been covered by computer-based visual simulation learning (Jensen et al., 2002; Chen et al., 2011). A review of these research findings revealed that learning performance can be enhanced if a visualized learning environment promotes learner interactions and allows manipulation (Jensen et al., 2002).

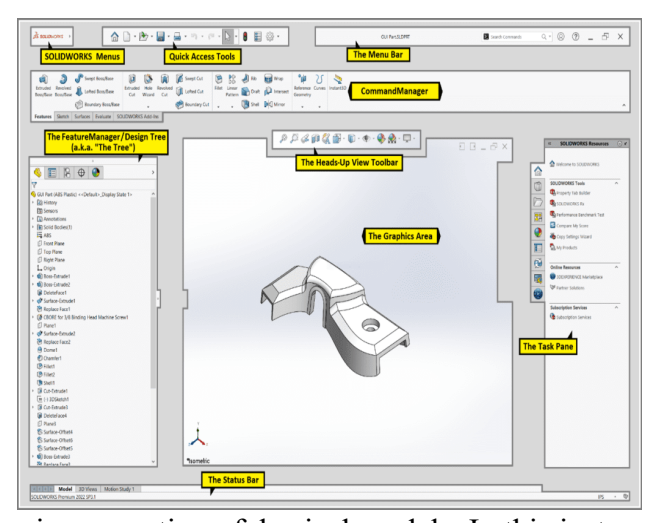
Solid Works is a complete 3D CAD design solution, providing the product design team with all the mechanical designs, verifications, motion simulations, data management, and communication tools that they need (Netshimbupfe et al., 2020) The Solidworks software is amechanical design automation application that lets designers quickly sketch ideas, experiment with features and dimensions, and produce models and detailed drawings. Solidworks adopts

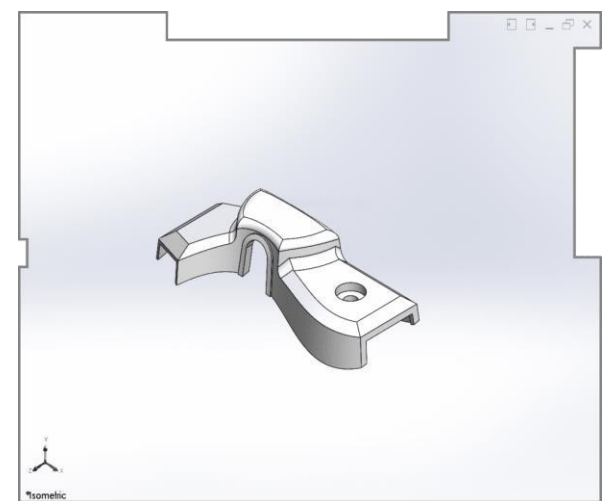
parametric modeling techniques and integrates part modeling, assembly modeling, and automatic generation of 2D engineering drawings and other functions. Numerous studies have emphasized the importance of software in engineering designs (Cekus et al., 2019; Eslami, 2017; Fialkova et al., 2023; Gajdoš & Tomek, 2022; Miclosina et al., 2021; Mitin & Sul'din, 2022; Saleh Al-Hammadi et al., 2022; Widiyanti et al., 2016; Yang et al., 2021; Zhetenbayev et al., 2023). They play a pivotal role in engineering designs, revolutionizing how engineers conceptualize, analyze, and create efficient, reliable, and innovative designs, accelerating progress in various engineering fields.

The Solidworks User Interface

Graphics Area

The traditional instructional model recommends bringing a physical model made of wood or plastic to the classroom to develop students' spatial imagination. This is done to familiarize students with solid models. Studies point to severe problems with the





incorporation ofphysical models. In this instance, a larger model is necessary for students to comprehend clearly. However, carrying big models is inconvenient. Furthermore, it was not possible to alter the models at will. As such, the traditional models could not meet the demands of mechanical design education. Using SolidWorks' handy modeling function, students cancreate a corresponding 3D model and edit it at leisure, providing an intuitive understanding ofpart design.

Mechanical design and drafting courses are essential courses for engineering majors. The emphasis of mechanical design and drawing courses is different for different majors. However, the primary purpose is to cultivate spatial imagination ability, guide students'robust modeling and 3D construction, and cultivate engineering and technical

personnel for enterprises with modern design philosophy and creative thinking ability. The simulation context empowers strong practical quality, aims to develop students' ability to think, analyze, and raise engineering questions, and improves their capacity in design processes.

Generally, mechanical engineering students in the National Institute of Construction Technology and Management, Edo State, Nigeria, are scheduled to take mechanical design and drawing courses in their early years. These courses serve as a connecting link betweenthe preceding and the following in cultivating students' professional ability. The teaching quality is directly concerned with the grasp of subsequent professional knowledge and even influences students' curriculum design and diploma projects. Moreover, mechanical design and drafting courses are firmly applied in future careers.

Strong spatial analysis and imaginative skills are required of engineering students. However, engineering design processes are challenging due to the student's insufficient learning infrastructure, space imagination, and mechanical part exposure. Traditional machine design learning requires students to transfer between 2D pictures and 3D objects, which is precisely why these courses are challenging. It would be highly beneficial if a bridge could be built to integrate the design and manufacturing processes seamlessly. Solidworks modeling creates a visual link and eliminates the need to convert 2D figures into 3D objects. Furthermore, it allows engineers to design components and assemblies in 3D accurately. As a result, it can potentially increase students' comprehension of figures and pique their interest.

# **Objective of the study**

SolidWorks software is a powerful 3D CAD (computer-aided design) program engineers use for design. It helps create models, drawings, and simulations quickly and easily. Thus, this study aims to explore the impact of Solidworks simulation software on mechanical

engineering students' design skills.

# Method

A quasi-experimental design was adopted. The participants comprised mechanical engineering students from the National Institute of Construction Technology and Management, Edo state, Nigeria. The samples (n = 47) were randomly drawn from the Mechanical Engineering Department. The experimental processes were conducted in the laboratory, and skills in mechanical design were determined with a structured questionnaire. The students were assigned to groups (A and B). while the A group was labeled the experimental group, the B group was considered the control group. The students participated in a pre-experiment survey by completing a questionnaire. Students' mechanical engineering design skills were evaluated in a preliminary test.

In the experiment, the experimental group was guided to use SolidWorks to create virtual components and assemblies in digital forms. Students grouped into small design teams could design and visualize their design options for evaluation. While creating virtual components, students could use the feature creation sequence to simulate the design process to visualize how to assemble the designed components. Students could assemble virtual components by the mating relations among components and understand how the components would be assembled for proper operation. On the other hand, group B represents the control condition, and mechanical design was taught using the traditional method. The post-test study was conducted similarly to the pre-test, except the questions were reshuffled. The data from the pre-test and post-test were subjected to data analysis.

# Result

**Table 1** shows the mean and standard deviation scores for the group.

		Pre-test	Post-test	
Group	N	Mean Standard Deviation	Mean Standard Deviation	Mean Gain

Experimental	24	43.17	10.54	50.19	13.68	7.02
Control	23	42.29	11.29	44.39	13.38	2.01
MD		0.88		5.08		

Table 1 shows that the mean in the pre-test study for experimental conditions is 43.17 while the mean in the pre-test for control conditions is 42.29, giving the pre-test mean difference of 0.88. The finding indicates no significant difference in the participants' mean scores on mechanical design skills. On the other hand, the post-test study reveals a mean of 50.19 for the experimental conditions and 44.39 for the control condition, with a mean difference of 5.08. The gain score for the two conditions was 7.02 and 2.01, respectively. Thus, the result shows that the experimental conditions improved mechanical design knowledge due to their exposure to the Solidworks software.

Table 2 shows a t-test comparison.

Source of variation	N	Mean	SD	df	t	Sig	
Experimental	24	50.19	13.68				
Control	23	44.39	13.38	185	7.328	000	

A t-test analysis was performed on the data to determine whether the Solidworks simulation software would increase students' mechanical design skills. The analysis established a significant difference between the experimental and control conditions on mechanical design skills MD = 5.08, t (185) = 7.328, p = .000. Thus, the result suggests that the Solidworks software might be used to improve student's mechanical design skills.

# **Discussion**

This study examined the impact of simulation software on mechanical design skills among mechanical engineering students at the National Institute of Construction Technology and

Management, Edo state, Nigeria. The result showed a significant difference between the students taught mechanical design processes using Solidworks simulation software and those prepared with conventional methods. For the pre-test and the post-test study conducted, the mean and standard deviation scores showed that exposing the students to Solidworks simulation software significantly influenced their mechanical design skills in the post-test study (M = 50.19, SD = 13.68) compared to the control group (M = 44.39, SD = 13.38). The probable explanation for this outcome is that SolidWorks helps to develop a visual representation of the concept in a 3D view. It displays the model in a particular orientation and scale. The drawing view can be annotated with dimensions, geometric tolerances, notes, and other annotations to represent the model with clarity. Thus, users can create parts and assemblies with precise relationships between components and analyze designs' static, kinematic, and dynamic behavior or evaluate the fatigue, thus providing the best-in-class responses.

# Conclusion

Solidworks potentially facilitates 3-D modeling, dynamically displaying the cutting process and generating virtual assembly and assembly exploded views. For mechanical engineering design, some instances demonstrate how SolidWorks can dynamically present complex issuesencountered in mechanical design and drafting while establishing a fundamental volume model. These issues include an exploded view, plane intersections with the primary volume model, and assembly. The finding supports the significance of Solidworks on the curriculum, students' aptitude for design and spatial imagination, their motivation to learn, and their capacity to recognize drawings. Utilizing Solidworks in the classroom has been demonstrated to substantially reduce the challenge of teaching and learning, boost student motivation, and contribute to successful teaching outcomes. The finding suggests regularly educating teachers in this area and integrating SolidWorks resources into the classroom.

#### References

Cekus, D., Gnatowska, R., Kwiatoń, P., & Šofer, M. (2019). Simulation research of a wind

- turbine using SolidWorks software. *Journal of Physics: Conference Series*, 1398(1). https://doi.org/10.1088/1742-6596/1398/1/012001
- Chen, Y., Wang, Y., & Chen, N. S. (2011). Computer-based visual simulation learning: Effects on science learning and cognitive load. Educational Technology & Society, 14(1), 54-65.
- Cohen, K., & Katz, R. (2015). Teaching mechanical design practice in academia. *Procedia CIRP*, 36. https://doi.org/10.1016/j.procir.2015.01.043
- Eslami, A. M. (2017). Integrating reverse engineering and 3D printing for the Manufacturing process. *ASEE Annual Conference and Exposition, Conference Proceedings*, 2017-June.https://doi.org/10.18260/1-2--28558
- Fialkova, E., Baronov, V., Slobodin, A., & Nechaev, K. (2023). SolidWorks flow simulation software potential in hydrodynamic processes analysis for cone vortex emulsion. *E3S Web of Conferences*, 402. https://doi.org/10.1051/e3sconf/202340203007
- Gajdoš, T., & Tomek, P. (2022). The use of an open-source FEA solver on a standard engineering problem. *Perner's Contacts*, 17(1). <a href="https://doi.org/10.46585/pc.2022.1.2295">https://doi.org/10.46585/pc.2022.1.2295</a>
- Jensen, E., Moorman, G., & Sonnemann, J. (2002). A fresh look at brain-based education: Teaching and learning from the inside out. Educational Leadership, 60(3), 30-34.
- Kuppuswamy, R., & Mhakure, D. (2020). Project-based learning in an engineering-design course Developing mechanical- engineering graduates for the world of work. *Procedia CIRP*, 91. https://doi.org/10.1016/j.procir.2020.02.215
- Miclosina, C.-O., Cojocaru, V., & Vela, D.-G. (2021). Friction Forces in Numerical Simulations of Kinematical Joints of Mechanical Systems. *Robotica & Management*, 26(1). https://doi.org/10.24193/rm.2021.1.2
- Mitin, E. V., & Sul'din, S. P. (2022). Stress-Strain State of Welds. *Russian Engineering Research*, 42(10). https://doi.org/10.3103/S1068798X22100173
- Netshimbupfe, A. F., Ali Abdalla, M. A. H., Erdem, B. D., Kassem, Y., & Camur, H. (2020). Solid Work simulation is a virtual laboratory concept that supports student mechanical
  - engineering learning. New Trends and Issues Proceedings on Humanities and SocialSciences, 7(3). https://doi.org/10.18844/prosoc.v7i3.5233
- Perez, V. V. B., Abreu, A. N., Khan, A. A., Guardia, L. E., Hasbún, I. M., & Strong, A. C. (2021). Mechanical Engineering Students' Perceptions of Design Skills Throughout a Senior Design Course Sequence. *ASEE Annual Conference and Exposition, Conference Proceedings*. https://doi.org/10.18260/1-2--36523
- Philippe, S., Souchet, A. D., Lameras, P., Petridis, P., Caporal, J., Coldeboeuf, G., & Duzan,

- H. (2020). Multimodal teaching, learning, and training in virtual reality: a review and case study. In *Virtual Reality and Intelligent Hardware* (Vol. 2, Issue 5). https://doi.org/10.1016/j.vrih.2020.07.008
- Saleh Al-Hammadi, A. S., Saidin, S., & Ramlee, M. H. (2022). Simulation Analyses Related to Human Bone Scaffold: Utilisation of Solidworks® Software in 3D Modelling and Mechanical Simulation Analyses. *Journal of Human-Centered Technology*, *I*(2). https://doi.org/10.11113/humentech.v1n2.28
- Widiyanti, Puspitasari, P., & Suyetno, A. (2016). The development of instructional materials mechanics of materials using Solidworks simulation software. *AIP ConferenceProceedings*, 1778. https://doi.org/10.1063/1.4965792
- Yang, M. L., Zhou, Y., Yang, X. W., Zhou, W. P., Qiang, R., Wang, J. L., & Zhu, K. (2021). The optimum design of the bracket support is based on SolidWorks. *Petrochemical Equipment*, 50(4). https://doi.org/10.3969/j.issn.1000-7466.2021.04.008
- Yavuzcan, H. G., & Gür, B. (2020). View of A Toolkit for Practice-Based Learning of Mechanisms in Industrial Design Education: An Application of a Method Combining Deductive and Inductive Learning. *Design and Technology Education: An International Journal*, 25(3).
- Zhetenbayev, N., Balbayev, G., Zhauyt, A., & Shingissov, B. (2023). Design and Performance of the New Ankle Joint Exoskeleton. *International Journal of Mechanical Engineering and Robotics Research*, 12(3). https://doi.org/10.18178/ijmerr.12.3.151-158

# RESPONSE OF ALPHA SPIN NANOPARTICLES AND DIFFERENT ORGANIC MANURE ON THE GERMINATION OF SESAME (SESAMUM INDICUM L.)

# Ogah, Godwin Omame, PhD

Department of Plant Science and Biotechnology, Federal University of Lafia.

Nasarawa State-Nigeria

\*Corresponding author's email address: ogahomams4@gmail.com

#### **ABSTRACT**

An experiment was carried out during the cropping season of 2023 in the Research and Experimental Field of the Botanical Garden of the Department of Plant Science and Biotechnology of Federal University of Lafia, Nasarawa State to investigate the influence of Alpha spin nanoparticles and different Organic manure on the germination of sesame (sesamum indicum). Sesame seeds were exposed to different levels of Alpha pin Nanoparticles at different time regime which include: 20minutes, 40minutes and 60minutes alongside the untreated (control). The land was treated with different organic manures which are Cow dung, Poultry droppings, Rice husk and Cow dung alongside untreated plot (control). The experiment was laid out in a Randomized Complete Block Design (RCBD) with three replications. The result from the study revealed that there was a significant difference (p < 0.05) in number of days to germinate while there were no significant differences (P > 0.05) in the percentage germination and seedling heights. The earliest number of days to germination was recorded under 60minutes of Alpha Spin nanoparticles (N3) and T3 (rice husk). The highest germination percentage was recorded under 40minutes (N2) with 0.63 and T3 (rice husk) with 0.68. The highest seedling height was recorded under control and T2 (poultry dropping). The result also showed that the alpha spin® nano particles reduced the number of days to germination, increased percentage germination against the control but it reduced the parameter for seedling height. Therefore, it could be concluded that Alpha spin® nanoparticles had little impact on the germination of sesame germination

**Keywords:** Alpha Spin, Nanoparticles, Organic Manure, Germination, Sesame

# INTRODUCTION

Sesame has been an important crop to Nigeria agriculture since its introduction to the country after the Second World War. It is an important component of Nigeria's agricultural exports (Abubakar et al., 1998). It is however, given little attention and there are relatively few companies involved in the trade. As a smallholder crop, often intercropped with other crops, the extent of cultivation is poorly known and there is little information on the morphological characterization, yields or productivity, genetic and environmental interaction. In Nigeria, sesame is widely grown in the northern and the central parts of the country as a minor crop. Since 1974, it has developed from being a crop of negligible importance to one of the major cash earner in its area of production (viz; Nasarawa, Borno, Gombe, Benue, Kogi, Kano, Jigawa, Plateau, Yobe, Katsina state as well as the FCT Abuja) (Abubakar, 1993). The current challenges of sustainability, food security and climate change are engaging researchers in exploring the field of nanotechnology as new source of key improvement for the agricultural sector. Several technological innovation have been employed in agricultural improvement of plants which have resulted in, hybrid variety, synthetic chemicals. Therefore, it will be of immense importance for researchers to seek in nanotechnology a new source of agricultural improvement (Paul, et al., 2019). Alpha spin optimizes the natural frequency as it can increase harmony in the body by stimulating vital life energy. Any contact with alpha-spin, the molecular structure will create smaller clusters that will make penetration and absorption easy by full optimizing the body's molecular and cellular functions via resonance and then forming a vortex that results in the expression of a quantum energy field which will exert its effect in the content of an organism's body (Gogos et al., 2012). Its functions include improvement of absorption and increase in hydrations, improve micro circulations. It can also be used to facilitate the flow of energy through reflexology frequency, through which it can improve plant growth, seed germination and extend the shelf life of fruits and vegetables (Abrehet et al., 2021). Nanotechnology has the potential to advance agricultural productivity through genetic improvement of plants, delivery of genes and drug molecules to specific sites at cellular levels, and nano-array based gene-technologies for gene expressions in plants and animals under stress conditions. The potential is increasing with suitable techniques and sensors being identified for precision agriculture, natural resource management, and early detection of pathogens and contaminants. Nanomaterials in agriculture aims in particular to reduce the amount of sprayed chemical products by smart delivery of active ingredients, minimize nutrient losses in fertilization and increase yields through optimized water and nutrient management (Gogos et al., 2012). The study investigates the effect of Alpha spin nanoparticles and organic manure on the germination of onion.

# MATERIALS AND METHODS

This research was carried out in the Botany Garden of Federal University of Lafia, Nasarawa State, located on latitude 80 35'N, longitude 8032'E altitude 181.53m above sea level with a mean temperature of 340c , relative humidity 0f 40-80 % and average day light of 9-12. It is located in the southern Guinea Savannah Region of North-central Nigeria. In the year 2022. Onion seeds (variety (ies)) were obtained from Nasarawa Agricultural Development Program (NADP). The treatments comprises of three levels of organic manure (cow dung (T1), poultry drop (T2) and rice husk (T3) and three levels of Alpha Spin nanoparticles at 20min (N1), 30mins (N2) and 60mins (N3) before planting while the untreated seeds were planted alongside the treated seeds and used as control. The experiment was laid out in a 42 factorial experiment in a Randomized Complete Block Design (RCBD) with three replications. Data were collected on the Number of Days to Germination, Number of Germinated Seeds, and Seedling Height (cm). The data were subjected to Two-Way analysis of variance (ANOVA) using GENSTAT version 17.0 software. Means were separated using least significant difference (LSD) at  $p \le 0.05$ .

#### RESULTS AND DISCUSSION

# **Number of Days to Germination**

The result shows that the differences in the number of days to germination among the plants exposed to alpha spin treatments are significant (Table 1). The number of days to germination of the control and N1 treatment do not significantly differ from each other whereas the N3 treatment was observed to have lowest (6.08) number of days to germination. Also as for the organic manure treatment, the differences in the number of days to germination are significant among the treatments with control having the highest (7.67) while T3 had the lowest (6.33) as indicated in Table 1. What is the implications of this findings / (results presented).

# **Percentage Germination of Seeds**

The effects of the organic manure treatments and alpha spin treatments on the percentage germination are not significant (Table 2). Although the plant exposed to N2 alpha spin treatment had the highest percentage germination (0.63) but not significantly different from that of the control, and other treatments. Similarly, the plants exposed to T3 organic manure treatment was observed to have the highest percentage germination which is not significantly different from the others as indicated in Table 2. You only presented the results but no discussion

# **Seedling Height**

 $LSD_{OM} = 0.45$ 

The effects of the organic manure treatments and alpha spin treatments on the seedling height are not significant (Table 3). The control plant had the highest seedling height but not significantly different from those of other alpha spin treatments. Similarly, the plants exposed to T2 organic manure treatment was observed to have the highest seedling height which is not significantly different from the control and others in Table 3. You only presented the results but no discussion.

Table 1: Number of days to germination of plant under Alpha spin and organic manure treatments

Alpha spin Treatments		Organic manure	Treatmen	Mean		
	T0	T1	T2	T3		
N0	9.00	7.67	7.67	6.00	7.58°	$LSD_{AS} = 0.45$
N1	8.00	7.67	7.00	7.00	$7.42^{c}$	LSD <sub>AS</sub> – 0.43
N2	7.33	6.67	6.67	6.33	$6.75^{b}$	
N3	6.33	6.00	6.00	6.00	$6.08^{a}$	
Mean	$7.67^{c}$	$7.00^{b}$	6.83 <sup>b</sup>	6.33 <sup>a</sup>		

Values with same superscript across same column or same row are not significantly different (P > 0.05)

Table 2: percentage germination of plant under alpha spin and organic manure treatments

Alpha	spin	Orga	nic manure T	reatments			
Treatments	_					Mean	
		T0	T1	T2	T3	_	
N0		0.48	0.72	0.52	0.57	$0.57^{b}$	

N1	0.52	0.24	0.54	0.53	0.46 <sup>b</sup>	$LSD_{AS} = 0.20$			
N2	0.74	0.63	0.61	0.55	$0.63^{b}$				
N3	0.49	0.61	0.45	0.68	$0.56^{b}$				
Mean	$0.56^{d}$	$0.55^{\rm d}$	$0.53^{d}$	$0.59^{d}$					
$LSD_{OM} = 0.20$									

Values with same superscript across same column or same row are not significantly different (P > 0.05)

Table 3: seedling height of plant under alpha spin and organic manure treatments

Alpha	spin	Organic n	nanure Treatr				
Treatments				Mean			
		T0	T1	T2	T3		
N0		8.43	8.50	11.23	9.30	$9.37^{d}$	
N1		8.63	8.43	8.43	6.73	$8.06^{d}$	$LSD_{AS} = 2.12$
N2		8.67	8.17	8.13	7.93	$8.23^{d}$	
N3		8.20	7.23	6.30	8.77	$7.63^{d}$	
Mean		8.48 <sup>e</sup>	$8.08^{\rm e}$	8.53 <sup>e</sup>	8.18 <sup>e</sup>		
	I	$LSD_{OM} = 2.1$	12				

Values with same superscript across same column or same row are not significantly different (P > 0.05).

#### Where:

Alpha Spin® Organic Manure N0= Control T0= Control

N1=20 Minutes T1= Cowdung

N2= 40 Minutes T2= Poultry Dropping

N3= 60 Minutes T3= Rice Husk

# CONCLUSION AND RECOMMENDATIONS

From the findings of this study, it could be concluded that Alpha spin nanoparticles and organic manure have impact on the number of days to germination of sesame, percentage germination and seedling height because there were significant differences between the exposed times in the number of days to germinations although there were no significant differences in the percentage germination and seedling heights respectively. Specifically, 60mins (N3) and Rice Husk (T3) treatments reduced the number of days to germination of the plant. This present study recommended that for better seedling height, percentage germination and number of days to germination, sesame seeds should be treated with Alpha spin nanoparticles at a longer period of time and organic manure such poultry droppings and rice husk should be used because the lowest number of days to germination, the highest percentage germination and the highest seedling heights were observed in the rice husk and poultry droppings treatments in combination with Alpha spin nanoparticles at 60minutes time of exposure.

## REFERENCES

Abubakar, S. S., Onlybe J.E., & Tologbone E.B. (1998). The role of extension research & the Information

dissemmnation in enhancing beniseed production and marketing by resource poor farmers in pre-conf. *Proceeding*. 1<sup>st</sup> National workshop on Beniseed, March 3-5, 1993 NCRI *baddegi* Nigeria 217

Abubakar, S. S. (1993). The Environment friendly Renewable Energy from sesame biodiesel. *Energy* 

Source part a-Recovery Utilization and Environmental Effects 32 (2), 189-196

Abrehet, F., Gebremeske, S., Peninah, N., Ngoda, Elizabeth, W., Kamau-Mbuthia, A. and Symon, M. (2021).

Value chain and microbiological Quality of crude sesame oil, a case study in Western Tigray, Ethiopia. *Food and Nutrition science vol.* 12.No.12. DOI:10.4236/fns.2021.1212096-24

- Gogos, A., Knauer, K. and Bucheli, T. D. (2012). Nanomaterials in plant protection and fertilization: Current state, foreseen applications and research priorities. *Journal of Agricultural Food Chemistry*. 60 pp. 9781-9792. DOI: 10.1021/if302154y.
- Paul, W., Yacouba, Z., Abdoul K., Hassan B., Franscois, L. and Et Michel, P. (2019). Combined Effects of Compost, Supraxone and Lambda-Super on Soil Microbial Activity under Pluvial Cultivation of Sesame (Sesamum indicum L.) in Burkina Faso. Journal of geoscience and environment protection. Vol. 12

. DOI: <u>10.4236/gep.2019.71009</u>

# Impact of Storage Practices on Fungal Infestation in Groundnuts: A Study from Nasarawa State, Nigeria

Dr. Pedro Akharenegbe

# Abstract

This study investigates the prevalence and diversity of fungi in stored groundnuts (Arachis hypogea) within Nasarawa State, Nigeria, an area once prominent in groundnut production but now facing challenges due to fungal contamination. The research involved sampling 300 groundnut specimens from various storage facilities across thirteen Local Government Areas (LGAs). The fungi were identified through macroscopic and microscopic examination, revealing ten fungal taxa: various Aspergillus species, Cladosporium spp., Emericella spp., Monascus ruber, Mucor species, Neosartorya fisheri, Penicillium spp., Rhizopus stolonifera, Trichoderma spp., and yeast. Rhizopus stolonifera was the most prevalent, particularly in Akwanga (60.9%), Nasarawa-Eggon (43.5%), and Wamba (39.1%). Aspergillus minisclerotigenes and Emericella spp. had the lowest occurrence, found only in Wamba (4.3%) with a cumulative frequency of 1.4%. Neosartorya fisheri and Monascus ruber were isolated solely from Kokona, with the lowest occurrence rates at 0.9% and 1.7%, respectively. The fungal contamination, particularly from Aspergillus and Penicillium species, produces harmful mycotoxins affecting food safety. This study underscores the need for improved storage practices and targeted interventions to mitigate fungal contamination and ensure the safety and economic viability of groundnut production in Nasarawa State.

# **INTRODUCTION**

Groundnuts, scientifically known as Arachis hypogea, are members of the Fabaceae family, are cultivated worldwide, and are also known as African nuts, monkey nuts, and peanuts (Salau et al., 2017). They thrive in regions across tropical, subtropical, and temperate zones, typically planted manually during the wet season (Abdulrahman et al., 2014). Following harvest, they are commonly stored in a range of traditional and modern storage facilities. However, such storage environments make them vulnerable to infestation by fungi, insects, and other microorganisms (Akharenegbe et al., 2022). Nigeria was once known as one of Africa's top groundnut producers and ranked among the world's largest producers of groundnuts serving as a significant source of foreign exchange for the country (Ogara et al., 2017). However, this prominence has waned due to the susceptibility of groundnut crops to fungal attacks, particularly during storage (Akharenegbe et al., 2022). This vulnerability poses a significant threat to the income of Nigerian farmers, who lack adequate storage facilities, improved crop varieties, and drying systems to mitigate moisture levels in the produce (Ogara et al., 2017). Sullivan (1984) reported that groundnut seeds are particularly susceptible to disease due to their abundance of stored nutrients, which serve as an ideal growth medium for various fungi, including Rhizopus spp., Penicillium spp., Aspergillus niger, and Aspergillus flavus. These Fungi also produce toxins as secondary metabolites, which are poisonous and carcinogenic to both humans and animals (Ogara et al., 2017). These mycotoxins fall into several classes, including aflatoxins, ergot alkaloids, amanitins, ochratoxins, cyclopiazonic acid, trichothecenes, citrinin, and slaframine. These harmful substances are mostly produced by fungi species such as Fusarium, Aspergillus, Alternaria, Penicillium, and Emericella. Food safety is a major international concern, as highlighted by the World Health Organization (WHO) in 2018. WHO reported a devastating economic burden due to the annual destruction of 25% or more of food crops in Africa caused by high mycotoxin incidence. In developing countries like Nigeria, numerous scientists have documented a high prevalence of fungi in groundnuts capable of producing mycotoxins (Akinnibosun and Osawaru, 2015; Ogara et al., 2017; Akharenegbe et al., 2022). In Nasarawa State, located in north-central Nigeria, data on the mycological diversity of stored groundnuts is limited. Therefore, this study aims to investigate and determine the fungal diversity present in stored groundnuts within Nasarawa State

# Methodology

# **Study Area and Design**

Thirteen Local Government Areas (LGAs) make up Nasarawa State, which is in north-central Nigeria: Obi, Awe, Keana, Lafia, Doma, Kokona, Karu, Keffi, Toto, Nasarawa, Akwanga, Nasarawa-Eggon, and Wamba. The Nigerian Investment Promotion Commission (NIPC) reported that commercial quantities of groundnuts are produced in each of these LGAs.

A combination of basic random sampling and deliberate sampling approaches was used to gather samples of groundnuts held for up to six months and to estimate the population number of local Hausa farmers who own mud barns, or "rumbu." The local government's agriculture departments and traditional authority helped facilitate this procedure.

# **Sampling**

A total of 300 stored groundnut samples, each weighing 4-5 kg, were obtained from different storage mud barns across the thirteen LGAs of Nasarawa State. The sample size was determined using the Raosoft sample size calculator. The samples were gathered, placed in coolers with ice packs, labeled, sealed, and packed in sterile plastic bags. They were then transported to the microbiology laboratory at the Federal University of Lafia for further examination.

# **Isolation and Identification of Fungal Isolates**

The procedure for the total heterotrophic fungus count is described by Akharenegbe et al. (2022). Ten grams of groundnuts that had been kept were homogenized in 90 milliliters of peptone water to create a stock suspension of the sample. The homogenate was then serially diluted ten times. Using a sterile glass spreader, 0.1 milliliters (mL) of each dilution was pipetted onto a potato dextrose agar plate. This process was repeated for duplication. The plates underwent a three- to five-day incubation period at 28 °C. Between 30 to 300 colonies were found on the agar surface, and each was counted and noted. Following the protocol described by Chuku et al. (2021), the fungal isolates were identified by first identifying them based on macroscopic characteristics such as shape, appearance, colour, conidia arrangement, and other vegetative structures; the fungi were then microscopically identified using a light compound microscope and lactophenol cotton blue stain, confirmed by specific identification keys.

# **RESULTS**

Table 1 showed the diversity of fungal species identified in the stored groundnut samples, including various Aspergillus species, Cladosporium spp., Emericella spp., Monascus ruber, Mucor species, Neosartorya fisheri, Penicillium spp., Rhizopus stolonifera, Trichoderma spp., and Yeast. Nasarawa-Eggon (43.5%), and Akwanga (60.9%). The least occurrence was observed for Aspergillus minisclerotigenes and Emericella spp., which were found only in Wamba LGA (4.3%), each contributing to a cumulative frequency of 1.4%. Table 2 showed the LGAs In the Nasarawa-West agricultural zone, Neosartorya fisheri, and Monascus ruber were isolated only from Kokona LGA, showing the least occurrence in the zone at 0.9% and 1.7%, respectively. Rhizopus stolonifera had the highest occurrence across all LGAs in the zone, at 82.6%. In the Nasarawa-South agricultural zone (table 3), Neosartorya fisheri (0.9%) and Trichoderma spp. (0.9%) had the lowest frequency of occurrence across the LGAs, while Rhizopus stolonifera showed the highest frequency at 58.2%, followed by Aspergillus niger at 45.7%.